https://doi.org/10.5194/acp-2020-262
Preprint. Discussion started: 16 April 2020

Atmospheric Chemistry and Physics Discussions

Climatological impact of the Brewer-Dobson Circulation on the N_2O budget in WACCM, a chemical reanalysis and a CTM driven by four dynamical reanalyses

Daniele Minganti[1], Simon Chabrillat[1], Yves Christophe[1], Quentin Errera[1], Marta Abalos[2], Maxime Prignon[3], Douglas E. Kinnison[4], and Emmanuel Mahieu[3]

[1]Royal Belgian Institute for Space Aeronomy, BIRA-IASB, Brussels, 1180 Belgium
[2]Universidad Complutense de Madrid, Madrid, Spain
[3]Institute of Astrophysics and Geophysics, University of Liège, 4000 Liège, Belgium
[4]National Center for Atmospheric Research, Boulder, CO, USA

Correspondence: Daniele Minganti (daniele.minganti@aeronomie.be)

Abstract.

The Brewer-Dobson Circulation (BDC) transports chemical tracers from the well-mixed tropical troposphere to the polar stratosphere, with many important implications for climate, chemistry, ozone distribution and recovery. Since the photochemical losses of nitrous oxide (N_2O) are well-known, model differences in its rate of change are due to transport processes that can be separated in the mean residual advection and the isentropic mixing terms in the Transformed Eulerian Mean (TEM) framework. Here the climatological impact of the stratospheric BDC on the long-lived tracer N_2O is evaluated through a comparison of its TEM budget in the Whole Atmosphere Community Climate Model (WACCM), a chemical reanalysis of the Aura Microwave Limb Sounder version 2 (BRAM2) and in a Chemistry-Transport Model (CTM) driven by four modern reanalyses (ERA-Interim, JRA-55, MERRA and MERRA2). The effects of stratospheric transport on the N_2O rate of change, as depicted in this study, have not been compared across this variety of datasets and never investigated in a chemical reanalysis. We focus on the seasonal means and climatological annual cycles of the two main contributions to the N_2O TEM budget: the vertical residual advection and the horizontal mixing terms.

The N_2O mixing ratio in the CTM experiments has a spread of approximately $\sim 20\%$ in the middle stratosphere, reflecting the large diversity in the mean Age of Air obtained with the same experiments. In all datasets the TEM budget is well-closed and the agreement between the vertical advection terms is qualitatively very good in the Northern Hemisphere, and good in the Southern Hemisphere except above the Antarctic region. The datasets do not agree as well with respect to the horizontal mixing term, especially in the Northern Hemisphere where horizontal mixing has a smaller contribution in WACCM than in the reanalyses. WACCM is investigated through three model realizations and a sensitivity test where gravity waves are forced differently in the Southern Hemisphere. The internal variability of the horizontal mixing in WACCM is large in the polar regions, and comparable to the differences between the dynamical reanalyses. The sensitivity test has a relatively small impact on the horizontal mixing term, but significantly changes the vertical advection term and produces a less realistic N_2O annual cycle above the Antarctic. In this region, all reanalyses show a large wintertime N_2O decrease, which is mainly due to

https://doi.org/10.5194/acp-2020-262
Preprint. Discussion started: 16 April 2020


Atmospheric Chemistry and Physics Discussions

horizontal mixing. This is not seen with WACCM, where the horizontal mixing term barely contributes to the TEM budget. While we must use caution in the interpretation of the differences in this region, where the reanalyses show large residuals of the TEM budget, they could be due to the fact that the polar jet is stronger and not tilted equatorward in WACCM compared with the reanalyses.

We also compare the inter-annual variability in the horizontal mixing and the vertical advection terms. As expected, the horizontal mixing term presents a large variability during austral fall and boreal winter in the polar regions . In the Tropics, the inter-annual variability of the vertical advection term is much smaller in WACCM and JRA-55 than in the other experiments. The large residual in the reanalyses and the disagreement between WACCM and the reanalyses in the Antarctic region highlight the need for further investigations on the modeling of transport in this region of the stratosphere.

1 Introduction

The stratospheric circulation is mainly characterized by the Brewer Dobson Circulation (BDC, Dobson et al., 1929; Brewer, 1949; Dobson, 1956), consisting in a slow upwelling in the Tropics from the troposphere into the stratosphere, followed by poleward transport and downwelling at higher latitudes in wintertime. For tracer-transport purposes the BDC is often divided into an advective component, the residual mean meridional circulation (hereafter residual circulation), and a quasi-horizontal two-way mixing which causes net transport of tracers, not of mass (Butchart, 2014).

The BDC is generated by Rossby waves propagating into the winter stratosphere (Charney and Drazin, 1961), which transfer angular momentum and force the stratosphere away from its radiative equilibrium. This departure from radiative equilibrium is balanced by a meridional (poleward) displacement of air masses, which implies tropical upwelling and extra-tropical downwelling (Holton, 2004). The residual circulation can be further separated in a shallow branch, i.e. an all year-round lower stratospheric two-cell system generated by synoptic-scale waves, and a winter-time deep branch in the higher part of the stratosphere generated by Rossby waves (Plumb, 2002).

The quasi-horizontal two-way mixing is generated by two-way transport due to the adiabatic motion of Rossby waves. In the stratosphere this motion is ultimately combined with the molecular diffusion which makes the total process irreversible (Shepherd, 2007). The two-way mixing is limited to a specific latitudinal region of the winter stratosphere, the 'surf zone' (McIntyre and Palmer, 1983). The mixing process homogenizes the tracer concentration in the surf zone and creates sharp tracer and Potential Vorticity (PV) gradients on its edges (in the tropics and at the polar vortex edge), indicating an inhibition of mixing. For this reason the tropics and the polar vortex edge are often called transport barriers (Shepherd, 2007).

Simulations by Chemistry Climate Model (CCM) predict a global BDC acceleration over the last decades and the twenty-first century due to global changes in the abundances of ozone depleting substances and greenhouse gases (Butchart et al., 2010; Hardiman et al., 2014; Palmeiro et al., 2014; Polvani et al., 2018), but these results cannot be evaluated easily because the BDC cannot be observed directly (Butchart, 2014). Observations of long-lived chemical tracers (e.g. H_2O, N_2O) are often used to derive estimates of the BDC (Butchart, 2014, and references therein). Yet, attempts to confirm the models' predictions with observation-derived datasets give contrasting results. Balloon-borne observations of SF_6 and CO_2 in the

https://doi.org/10.5194/acp-2020-262
Preprint. Discussion started: 16 April 2020


Atmospheric Chemistry and Physics Discussions

Northern Hemisphere (NH) middle latitudes show a non-significant trend in the past decades (Engel et al., 2009, 2017). Studies over shorter periods and using other tracers or temperature observations show significant evidence of a changing BDC in the boreal lower stratosphere (Ray et al., 2014; Hegglin et al., 2014; Haenel et al., 2015).

A number of studies on the possible BDC changes compared observations, reanalyses and climate models (Mahieu et al., 2014; Garfinkel et al., 2017; Stiller et al., 2017; Chabrillat et al., 2018). The difficulty to derive significant trends in the BDC can be partly attributed to the spatial and temporal sparseness of the observations, together with its large dynamical variability and the uncertainty of trends derived from non-linearly increasing tracers (Garcia et al., 2011; Hardiman et al., 2017). Furthermore the observational datasets cannot discriminate between the separate effects of residual circulation and mixing. This separation turns out to be important in the BDC change studies in climate models (Garny et al., 2014; Ploeger et al., 2015; Eichinger et al., 2019).

In this study we use nitrous oxide (N_2O) as a tracer to study the BDC. N_2O is continously emitted in the troposphere (with larger abundances in the NH), and transported into the stratosphere where it is destroyed by photodissociation and, to a lesser extent, by reaction with $O(^1D)$. The estimated lifetime of N_2O is approximately 120 years, which makes it an excellent long-lived tracer for transport studies in the middle atmosphere (Brasseur and Solomon, 2006; Seinfeld and Pandis, 2016).

We use the Transformed Eulerian Mean (TEM) (Andrews et al., 1987) analysis to separate the local rates of change of N_2O due to transport and chemistry (Randel et al., 1994). The transport term can be further separated into the contribution of isentropic mixing and residual advection (Abalos et al., 2013; Tweedy et al., 2017). The isentropic mixing and the residual advection can be separated in their horizontal and vertical contributions. Here the horizontal mixing and the vertical advection are investigated, because their magnitude is larger than the vertical mixing and the meridional residual advection in most of the stratospheric N_2O budget (Abalos et al., 2013). We use the Whole Atmosphere Community Climate Model version 4 (WACCM, Garcia et al., 2017) to simulate the N_2O TEM budget in the stratosphere for the 2005-2014 period, and we compare the results with those obtained from several reanalysis datasets.

Dynamical reanalyses merge dynamical atmospheric observations (e.g. surface pressure, wind, temperature) with a global forecast model using an assimilation scheme to offer the best reproduction of the past climate. They provide a multivariate, consistent record of the global atmospheric state. Reanalyses are made using different assimilation methods and forecast models, and they are often compared among each other and with CCMs (Fujiwara et al., 2017; Cameron et al., 2019). While dynamical reanalyses do not assimilate observations of chemical compounds, chemical reanalyses achieve this step, and can be used to evaluate CCMs or study differences between instruments using the reanalysis as a transfer tool (Inness et al., 2013; Davis et al., 2016).

The dynamical reanalyses are used here to drive 4 different simulations of the Belgian Assimilation System for Chemical ObsErvation (BASCOE) Chemistry-Transport Model (CTM) (Chabrillat et al., 2018). Namely we consider: the European Centre for Medium-Range Weather Forecasts Interim Reanalysis (ERA-Interim), the Japanese 55-year Reanalysis (JRA55), the Modern-Era Retrospective analysis for Research and Applications version 1 (MERRA), and version 2 (MERRA2). WACCM4 is also compared to a chemical reanalysis of Aura Microwave Limb Sounder (MLS) using the BASCOE assimilation system driven by the ERA-Interim reananlysis (BRAM2, Errera et al., 2019).

https://doi.org/10.5194/acp-2020-262
Preprint. Discussion started: 16 April 2020


Atmospheric Chemistry and Physics Discussions

WACCM has been widely used for studies of tracers transport in the stratosphere and upper troposphere based on the TEM analysis (e.g. Abalos et al., 2013, 2017). CTMs driven by dynamical reanalyses are often used to investigate Age of Air (e.g. Chabrillat et al., 2018; Ploeger et al., 2019). Chemical reanalyses have not been used to study stratospheric tracer transport in the TEM framework to our knowledge. In this study we analyze and compare the effect of transport on the stratospheric N_2O using the state-of-the-art CCM WACCM, together with the BASCOE CTM driven by a variety of dynamical reanalyses, and the BRAM2 chemical renalysis.

In Section 2 we describe the datasets used in the study and the TEM analysis of N_2O. In Section 3.1 we analyse the seasonal mean patterns of the TEM budget in the different datasets and their differences. In Sections 3.2 and 3.3, respectively, the mean annual cycle and variability of the N_2O TEM budget terms are studied, with a focus on the differences between the datasets. Section 4 discusses the results pointing to the possible causes of disagreements and section 5 concludes the study with a summary of our findings and possible future research.

2 Data and methods

2.1 WACCM

WACCM (Garcia et al., 2017) is the atmospheric component of the Community Earth System Model version 1.2.2 (Hurrell et al., 2013), which has been developed by the U.S. National Center of Atmospheric Research. It is the extended version of the Community Atmosphere Model version 4 (CAM4, Neale et al., 2013).

We ran one realization of the public version of WACCM (hereafter WACCM4, Marsh et al., 2013), that we downloaded at https://svn-ccsm-models.cgd.ucar.edu/cesm1/release_tags/cesm1_2_2cesm1_2_2. In this study we also use 3 realizations of the REF-C1 simulation used in the SPARC (Stratosphere-troposphere Processes And their Role in Climate) Chemistry-Climate Model Initiative (CCMI, Morgenstern et al., 2017). The CCMI experiments, hereafter WACCM-CCMI, differ from WACCM4 for the modified gravity waves parameterization and the updated heterogenous chemistry (Garcia et al., 2017). The inclusion of WACCM4 allows us to make a sensitivity test for the impact of the modified gravity waves parameterization on the simulation of the N_2O trasport (see Sect. 4). We consider the 2005-2014 period to allow a fair comparison with the BRAM2 dataset (see Sec. 2.3). WACCM has a longitude-latitude grid of 2.5°x1.9°and 66 vertical levels ranging from the surface to about 140 km altitude. The vertical coordinate is hybrid-pressure, i.e. terrain-following below 100 hPa and purely isobaric above. The vertical resolution depends on the height: it is approximately 3.5 km above 65 km, 1.75 km around the stratopause (50 km), 1.1-1.4 km in the lower stratosphere (below 30 km), and 1.1 km in the troposphere. The time step for the physics in the model is 30 minutes.

The physics of WACCM is the same as CAM4 and the dynamical core is a finite volume with a horizontal discretization based on a conservative flux-form semi Lagrangian (FFSL) scheme (Lin, 2004). The gravity wave parameterization accounts for momentum and heat deposition separating orographic and non-orographic sources. The orographic waves are modified according to Garcia et al. (2017), while non-orographic waves are parameterized depending on the convection and the fronto-genesis occurrence in the model (Richter et al., 2010).

https://doi.org/10.5194/acp-2020-262
Preprint. Discussion started: 16 April 2020


Atmospheric Chemistry and Physics Discussions

The WACCM versions considered here are not able to generate the Quasi Biennial Oscillation (QBO, see e.g. Baldwin et al., 2001) internally, forcing it instead by a relaxation of stratospheric winds to observations in the Tropics (Matthes et al., 2010). The solar forcing uses the Lean et al. (2005) approach.

WACCM includes a detailed coupled chemistry module for the middle atmosphere based on the Model for Ozone and Related Chemical Tracers, version 3 (MOZART-3) (Kinnison et al., 2007; Marsh et al., 2013). The species included within this mechanism are contained within the O_x, NO_x, HO_x, ClO_x and BrO_x chemical families, along with CH_4 and its degradation products. In addition 20 primary non-methane hydrocarbons and related oxygenated organic compounds are represented along with their surface emission. There is a total of 183 species and 472 chemical reactions; this includes 17 heterogeneous reactions on multiple aerosol types, i.e. sulfate, nitric acid trihydrate, and water-ice. In WACM-CCMI the heterogeneous chemistry is updated by Solomon et al. (2015).

2.2 BASCOE CTM

The BASCOE data assimilation system (Errera et al., 2019) is built on a Chemistry-Transport Model which consists in a kinematic transport module with the FFSL advection scheme (Lin and Rood, 1996) and an explicit solver for stratospheric chemistry, comprising 65 species and 243 reactions (Prignon et al., 2019). The transport module requires on input only the surface pressure and horizontal wind fields from reanalyses, as it relies on mass continuity to derive vertical mass fluxes. Similar to Chabrillat et al. (2018), the model is driven by four different reanalysis datasets on a common, low-resolution latitude–longitude grid (2.5°x2°) but keeping their native vertical grids. In this way we avoid any vertical regridding and the intercomparison explicitly accounts for the different vertical resolutions.

The four input reanalyses are part of the SPARC Reanalysis Intercomparison Project (S-RIP) which is a coordinated intercomparison of all major global atmospheric reanalyses. They are described in Fujiwara et al. (2017): the European Centre for Medium-Range Weather Forecasts Interim Reanalysis (ERA-Interim, hereafter ERAI; Dee et al., 2011), the Japanese 55-year Reanalysis (JRA55; Kobayashi et al., 2015), the Modern-Era Retrospective analysis for Research and Applications (MERRA; Rienecker et al., 2011) and its version 2 (MERRA2; Gelaro et al., 2017). ERAI and JRA55 have 60 levels up to 0.1 hPa while MERRA and MERRA2 have 72 levels up to 0.01 hPa. The CTM time step is set to 30 minutes. For this work the BASCOE CTM provided daily mean outputs over the 2005-2014 period as for the WACCM experiment.

2.3 BASCOE Reanalysis

The TEM diagnosis is also applied to N_2O assimilated fields from the BASCOE Reanalysis of Aura MLS, version 2 (BRAM2, Errera et al., 2019) which covers the period August 2004-August 2019. For BRAM2, BASCOE is driven by dynamical fields from ERA-Interim, with a horizontal resolution of 3.75°x2.5°longitude-latitude. The vertical grid is represented by 37 hybrid-pressure levels which are a subset of the ERA-Interim 60 levels.

In BRAM2, N_2O profiles from MLS version 4 standard product has been assimilated within the 0.46-68 hPa pressure ranges (Livesey et al., 2015). This product is retrieved from the MLS 190 GHz radiometer instead of the 640 GHz radiometer in earlier MLS version. The 640 GHz radiometer, which provided a slightly better quality retrieval down to 100 hPa, ceased to

https://doi.org/10.5194/acp-2020-262
Preprint. Discussion started: 16 April 2020

Atmospheric Chemistry and Physics Discussions

be delivered after August 2013 because of instrumental degradation in the band used for that retrieval. To avoid any artificial discontinuity due to switching from one product to the other in August 2013, BRAM2 has assimilated the 190 GHz N_2O during the whole reanalysis period.

BRAM2 N_2O has been validated against several instruments with a general agreement between 15 % depending on the instrument and the situation of interest and between 3 and 68 hPa (see Errera et al., 2019). It is not recommended to use BRAM2 N_2O reanalysis outside these pressure ranges. BRAM N_2O is also affected by a small drift of around -4 % between 2005 and 2015 (see also Froidevaux et al., 2019; Livesey, in preparation).

2.4 TEM diagnostics

For atmospheric tracers the TEM analysis (Andrews et al., 1987) allows to separate the local change of a tracer χ in terms due to transport and chemistry (Eq. (1)).

$$\bar{\chi}_t = -\bar{v}^*\bar{\chi}_y - \bar{w}^*\bar{\chi}_z + e^{z/H}\boldsymbol{\nabla}\cdot\boldsymbol{M} + \bar{S}, \tag{1}$$

where $\boldsymbol{M}$ is the eddy flux vector, defined as:

$$M^{(y)} \equiv -e^{-z/H}(\overline{v'\chi'} - \overline{v'\theta'}\bar{\chi}_z/\bar{\theta}_z), \tag{2a}$$

$$M^{(z)} \equiv -e^{-z/H}(\overline{w'\chi'} + \overline{v'\theta'}\bar{\chi}_y/\bar{\theta}_z), \tag{2b}$$

and v^* and w^* are the meridional and vertical components of the residual mean meridional circulation, and defined respectively as:

$$\bar{v}^* \equiv \overline{v} - e^{z/H}(e^{-z/H}\overline{v'\theta'}/\overline{\theta}_z)_z, \tag{3a}$$

$$\bar{w}^* \equiv \overline{w} + (acos\phi)^{-1}(cos\phi\overline{v'\theta'}/\overline{\theta}_z)_\phi. \tag{3b}$$

Where $\bar{v}$, $\bar{w}$ and $\bar{\theta}$ are respectively the Eulerian zonal-mean meridional and vertical velocities and the potential temperatures, ϕ is the latitude, and S is the net rate of change due to chemistry $\bar{S} = \bar{P} - \bar{L}$, where $\bar{P}$ and $\bar{L}$ are respectively the zonal-mean chemical production and loss rates. Overbar quantities represent zonal mean fields, primed quantities the departures from the zonal mean, and subscripts denote derivatives. Meridional derivatives are evaluated in spherical coordinates and vertical derivatives with respect to log-pressure altitude $z \equiv -Hlog_e(p/p_s)$, with $p_s = 10^5 Pa$ and $H = 7km$.

Hence transport is separated into the advection due to the residual circulation (first 2 terms on the right-hand side (RHS) of Eq. (1)) and the irrevesible quasi-horizontal isentropic eddy mixing $e^{z/H}\boldsymbol{\nabla}\cdot\boldsymbol{M}$ (third term on the RHS of Eq. (1)).

In order to better understand the role of each term in the N_2O balance it is useful to separate the components of the vector **M** and rearrange the terms of Eq. (1):

$$\bar{\chi}_t = A_y + M_y + A_z + M_z + (\bar{P} - \bar{L}) + \bar{\epsilon}, \tag{4}$$

https://doi.org/10.5194/acp-2020-262
Preprint. Discussion started: 16 April 2020


Atmospheric Chemistry and Physics Discussions

where:

$$A_y = -\bar{v}^* \bar{\chi}_y, \tag{5a}$$

$$M_y = e^{z/H} cos\phi^{-1} (M^{(y)} cos\phi)_y, \tag{5b}$$

$$A_z = -\bar{w}^* \bar{\chi}_z, \tag{5c}$$

$$M_z = e^{z/H} (M^{(z)})_z, \tag{5d}$$

with A_y representing the meridional residual advection, M_y the horizontal transport due to eddy mixing, A_z the vertical residual advection and M_z the vertical eddy mixing (all expressed in $\mathrm{ppbv\,day^{-1}}$). It is important to note that the total mixing term ($M_y + M_z$) includes not only the effects of irreversible mixing, but also some effects of the advective transport which are not resolved by the residual advection (Andrews et al., 1987; Holton, 2004).

Before any TEM calculation all the input fields are interpolated to constant pressure levels from the hybrid-sigma coefficients, hence retaining the original vertical grid of each dataset. Each derivative is computed using a centered differences method.

In addition to the physical TEM terms (Eq. (1)), it is necessary to include an additional term on the RHS of Eq. (4): the residual term ϵ. It is the difference between the actual rate of change of χ (LHS of Eq. (4)) and the sum of all the transport and chemical terms of the TEM budget.

The non-zero residual has several causes (Abalos et al., 2017). The TEM calculations for WACCM rely on a diagnostic variable which is not used to advect the tracers, because the model is based on a Finite Volume dynamical core (Lin, 2004). Furthermore in WACCM an implicit numerical diffusion is added to the transport scheme in order to balance the small-scale noise without altering the large-scale. This numerical diffusion is not included in the TEM budget and is larger in regions with large small-scale features, i.e. regions where gradients are larger/stronger (Conley et al., 2012). All TEM calculations are done using daily mean data, while WACCM and BASCOE both run with a much smaller timestep of 30 minutes. Finally, the daily mean fields are interpolated from their native hybrid-sigma levels to constant pressure levels prior to the TEM analysis. This could lead to numerical errors in the lower stratosphere. For WACCM-CCMI the TEM budget is computed for each realization, allowing the examination of both the multi-model mean (e.g. for seasonal means) or the model envelope (e.g. for line plots). In order to validate our $\mathrm{N_2O}$ TEM budget, we reproduced the findings reported in Tweedy et al. (2017, Fig. 7) with WACCM-CCMI, and we noticed similar results (not shown).

Dynamical reanalyses provide realistic temperature and winds in the stratosphere, but can lead to different representation of large-scale transport (e.g. Chabrillat et al., 2018). Note that the TEM quantities are not directly constrained by observations. The upwelling velocity $\bar{w}^*$ can vary considerably in the dynamical reanalyses (Abalos et al., 2015). In the rest of the paper we will assume that the BASCOE reanalysis BRAM2 provides the best available approximation of the TEM budget for $\mathrm{N_2O}$, at least where the residual is smaller than the vertical advection and horizontal mixing terms. This assumption relies on the combination in BRAM2 of dynamical constraints from ERA-Interim with chemical constraints from MLS (Errera et al., 2019).

https://doi.org/10.5194/acp-2020-262
Preprint. Discussion started: 16 April 2020


Atmospheric Chemistry and Physics Discussions

In Figs. 1 and 2 we show the N_2O TEM budget terms at 15 hPa for all the datasets for the December-January-February (DJF) and June-July-August (JJA) means respectively. It is important to make this seasonal distinction because the TEM quantities are the strongest in the winter hemisphere (see Sect. 1).

The choice of the 15 hPa (around 30 km) level is due to the large differences that can be found between WACCM-CCMI, BRAM2, and the CTM runs, and the better assimilation of meteorological observations at this altitude with respect to higher levels (Manney et al., 2003).

Figure 1 shows the N_2O TEM budget in DJF at 15 hPa for the considered datasets. The Tropics are characterized by a N_2O increase due to the upwelling, balanced by a decrease mostly due to the chemical loss and, to a smaller extent, meridional advection. In the northern tropics the N_2O decrease due to horizontal mixing is clearly compensated by A_y in WACCM-CCMI (Fig. 1(a)), while for the reanalysis datasets a positive residual term arises because A_y is not sufficient to do so. At the higher latitudes the main terms contributing to the N_2O TEM budget are the positive horizontal mixing term in the N_2O increase, and the negative vertical advection and vertical mixing terms for the N_2O decrease in all the datasets, with negligible contributions from the other terms (except for the residual term which plays a minor role especially in the reanalyses).

Figure 2 is the same as Fig. 1 but for the JJA season. In the northern Tropics the main terms contributing to the N_2O budget are the increase due to the vertical advection and the loss due to chemistry. In the southern tropics the pattern is noisier, with a general balance between the M_y and A_y, while, especially in the reanalyses, A_z and the residual terms play a minor role. In the southern mid-latitudes a large contribution is due to the negative A_z and the positive M_y; the residual term plays a role in the balance of M_y in the reanalyses, especially in BRAM2 (Fig. 2(f)). In the Southern polar region the N_2O distribution is affected mostly by a decrease due to the horizontal mixing and to the vertical advection to a smaller extent. M_z plays a role in decreasing N_2O mostly around 60° S in the reanalyses, while it increases N_2O in the WACCM-CCMI simulations. South of 60° S the WACCM-CCMI simulations do not show large contribution to the N_2O budget for any of the terms, while the raenalyses show a consistent N_2O decrease due to the horizontal mixing and balanced by a positive residual term. Such differences in the importance of M_y and the large residual term make the TEM analysis less robust in the antarctic region.

3 TEM balances

3.1 Cross sections

Figures 3 and 4 show respectively the DJF and JJA means of three contributions to the N_2O TEM budget, namely horizontal mixing M_y, vertical advection A_z and residual term ϵ, for WACCM-CCMI, JRA55, MERRA2 and BRAM2. The CTM results with MERRA and ERAI are not shown because they are analogous to those obtained with MERRA2. In the case of WACCM-CCMI the seasonal means were computed separately for each realization and we verified that the multi-model means show the same features as the individual realizations. We first compare the contribution of vertical advection across the datasets. The tropical upwelling increases the abundance of N_2O mostly in the mid-high stratosphere (between 1 and 15 hPa) with the maximum contribution in the summer tropics, while the downwelling decreases it mostly in the wintertime extratropics in the middle and low stratosphere (between 5 and 100 hPa). This reflects the path followed by the deep branch of the BDC (Birner

https://doi.org/10.5194/acp-2020-262
Preprint. Discussion started: 16 April 2020


Atmospheric Chemistry and Physics Discussions

and Bönisch, 2011). During the DJF season these features are very similar across all datasets (Fig. 3) but noticeable differences appear during the JJA season (Fig. 4): the tropical upwelling has a clearer secondary maximum in the reanalyses (e.g. JRA55, MERRA2) than in WACCM-CCMI, and the extra-tropical downwelling extends to the South Pole in WACCM-CCMI and JRA55 while it is mostly confined to the mid-latitudinal surf zone in the four other reanalyses.

This surf zone is also characterized by strong mixing and delimited by transport barriers which appear here as intense gradients of M_y in the winter hemisphere (middle columnns of Figs. 3 and 4). In the wintertime NH the patterns of M_y are similar in all datasets (Fig. 3), but the effect of irreversible mixing on N_2O is stronger in the reanalyses than in WACCM-CCMI. The residual term in the reanalyses (Fig. 3(f),(i),(l)) presents larger values in correspondence to the transport barriers in the middle stratosphere, that tend to cancel the M_y contribution.

In the JJA season there is an important disagreement in M_y between WACCM-CCMI and the reanalyses (middle column of Fig. 4). The transport barrier at the polar vortex edge (strong vertical gradients of zonal wind) can be clearly seen in the reanalyses as weak mixing (grey vertical lines) (Haynes and Shuckburgh, 2000a), but WACCM-CCMI has strong mixing there with very positive values of M_y. Inside the Antarctic vortex and above 20 hPa, the reanalyses show a negative contribution of horizontal mixing to the N_2O budget whereas this contribution is very small in WACCM-CCMI. A physical interpretation of these patterns is not straightforward because the TEM budget is not fully closed in the SH polar regions in the reanalyses as the residual term is large (right column of Fig. 4). The largest residual is encountered with BRAM2 in the outer part of the antarctic vortex. In the next section we focus on a single level in the middle stratospheric to investigate quantitatively the disagreement between WACCM-CCMI and the reanalyses, accounting for the largest residual term (i.e. BRAM2).

3.2 Climatological seasonal cycles

In this section we show the monthly mean climatological annual cycles of the N_2O mixing ratio, and two transport terms that contribute to its time derivative: M_y and A_z, for all the datasets at 15 hPa (around 30 km, Figs. 5 and 6). As shown in the previous figures this level corresponds to the maximum values of both M_y and A_z. The cycles are shown separately in each hemisphere for three latitude bands corresponding to the Tropics (0°-20°), the surf zones (40°-60°) and the polar regions (60°-80°). The subtropical barriers are not shown because of the large latitudinal gradients of M_y and A_z in these regions that would hinder the interpretation of their means. For WACCM-CCMI we show the envelope of the three model realizations in order to evaluate the role of the internal variability and its relative importance for each month and latitude band. The color codes for the four CTM simulations follow the conventions of S-SRIP (Fujiwara et al., 2017). BRAM2 is depicted with a black line and symbols, as usually done for observations, because it is constrained by both dynamical and chemical observations. Since the N_2O mixing ratio in BRAM2 has been evaluated with a 15% uncertainty at 15 hPa (Errera et al., 2019), this is highlighted by a dark grey regions in top rows of Figs. 5 and 6). The light grey shading around the BRAM2 cycles represents the uncertainty arising from the residual term in the TEM budget, i.e. it is entirely interpreted first as an uncertainty on A_z and then as an uncertainty on M_y in order to remain cautious.

We first investigate the N_2O mixing ratio in the SH. In the Tropics (Fig. 5(c) and 6(a)), using the BRAM2 reanalysis of Aura MLS as reference, JRA55 and WACCM-CCMI agree very well, while ERAI, MERRA2 and MERRA underestimate the

https://doi.org/10.5194/acp-2020-262
Preprint. Discussion started: 16 April 2020


Atmospheric Chemistry and Physics Discussions

N_2O mixing ratio. WACCM-CCMI exhibits nearly no annual cycle, which is in clear disagreement with the reanalyses. In the antarctic region (Fig. 5(a)) the annual mean agrees well among all the datasets, but the springtime increase is smaller in all the simulations than in BRAM2. In all the latitude bands the WACCM-CCMI simulations are not outliers compared to the reanalyses, while, regarding A_z and M_y, they differ with the reanalyses, especially in the polar regions. This will be discussed in Section 4.

We then investigate the contribution from vertical advection in the SH, starting from the Tropics. A_z in the 20°-0 S latitudinal band (Fig. 5(f)) is positive all year round showing the effect of tropical upwelling. As expected, the largest values are in the boreal late-fall and winter (Seviour et al., 2012). The datasets show a general agreement, but WACCM-CCMI underestimates A_z by up to $\sim 20\%$ in January and JRA55 overestimates it up to $\sim 50\%$ in November. In the Southern mid-latitudes (Fig. 5(e)) A_z is negative in all seasons except during summer and there is again a good agreement among the datasets except for WACCM-CCMI and JRA55. These two datasets appear to have a purely annual cycle in this region, while the other four show a semi-annual component. The strongest contributions are reached in September for all reanalyses, with JRA55 almost twice more negative than the other ones. WACCM-CCMI, on the other hand, reaches its strongest contribution three months earlier (June) with A_z twice larger than obtained with BRAM2. In the antarctic region (Fig. 5(d)) A_z shows the effect of downwelling on N_2O during most of the year. Here again JRA55 and WACCM-CCMI are outliers: both present stronger A_z contributions in fall and winter, especially WACCM-CCMI reaching values three times lower than BRAM2 in early winter. While this strong disagreement is questioned by the large residuals, we note that all the reanalyses confirm it except for JRA55.

We now turn to the contribution from the horizontal mixing in the same hemisphere (Fig. 5 bottom row). In the Tropics (Fig. 5(i)) M_y shows a N_2O decrease from May to October (when N_2O is transported to the middle latitudes), and a near-zero contribution in the rest of the year, generally common in all the considered datasets. The BRAM2 uncertainty is smaller than for the polar region (Fig. 5(g)) and middle latitudes (Fig. 5(h)) confirming the better performances of the TEM analysis outside the high latitudes. It is yet comparable with M_y, because its contribution is quite small in this region, where the largest dynamical term is A_z (Fig. 5(f)). In the southern mid-latitudes (Fig. 5(h)) M_y increases throughout the winter, reflecting the mixing associated to the surf zone, and peaks in the early spring (September). During summer and early fall M_y does not contribute significantly to the TEM budget, and in Novemeber M_y reaches negative values which are comparable to the residual term. In WACCM-CCMI M_y starts increasing in February, i.e. two months earlier than the ranalyses, and the values reamain twice larger during fall and winter, but they stop increasing in August, i.e. one month earlier than the reanalyses. In the antarctic region (Fig. 5(g)) M_y is very differt among the datasets: in BRAM2 it contributes to the N_2O decrease during fall and winter, with the strongest contribution in July, but with the CTM simulations this contribution is twice weaker, while in WACCM-CCMI the horizontal mixing has almost no effect on N_2O. During spring all the datasets show similarly positive values for M_y, with WACCM-CCMI presenting a large internal variability. As already mentioned, the TEM analysis suffers from large residuals in the antarctic region. Yet we note that the disagreement between WACCM-CCMI and BRAM2 is significant, because in fall and winter the envelope of WACCM-CCMI realizations falls completely outside of the possible BRAM2 values when accounting for the residual.

https://doi.org/10.5194/acp-2020-262
Preprint. Discussion started: 16 April 2020


Atmospheric Chemistry and Physics Discussions

In the NH (Fig. 6) the vertical range for A_z and M_y is extended with respect to the SH because of the larger values of the TEM terms above the Arctic, and the x axis is shifted by six months to better show the boreal winter. With regard to the N_2O mixing ratio, (Fig.6 upper row) WACCM-CCMI and the CTM driven by JRA55 are in good agreement with BRAM2, while ERAI, MERRA2 and MERRA underestimate it.

In the tropics, A_z (Fig. 6(d)) shows the effect of the upwelling that transports N_2O from lower levels all year round, and in the middle latitudes (Fig. 6(e)) the wintertime downwelling to the lower stratosphere. The agreement is very good among the datasets in both latitude bands. The arctic region (Fig. 6(f)) is also characterized by the wintertime downwelling, which peaks in January, with JRA55 and ERAI showing a larger contribution ($\sim 30\%$ difference) than the other datasets.

Finally we consider the contribution of the horizontal mixing in the NH (Fig. 5 bottom row). In the Tropics from Novermber to April (Fig. 6(g)) M_y is negative and presents a marked seasonality in the reanalyses that is much weaker in WACCM-CCMI. In the middle latitudes (Fig. 6(h)) the strong horizontal mixing in the surf zone tends to increase N_2O during winter. The reanalyses show a large spread, with values reaching ~ 1.5 ppbv day^{-1} in BRAM2 and ~ 0.9 ppbv day^{-1} in the MERRA runs, while WACCM-CCMI presents a large underestimation with respect to the reanalyses. In the arctic region (Fig. 6(i)) we note a seasonal cycle twice stronger than in the mid-latitudes. Large discrepancies characterize this region: BRAM2 delivers the largest value among all datasets, the CTMs agree for a smaller contribution in late winter and spring, and WACCM-CCMI significantly underestimates M_y as evaluated by all reanlyses. We also note that M_y in WACCM-CCMI has a larger internal variability in the Arctic than in the other regions.

3.3 Interannual variability of the seasonal cycles

After reporting on the climatological annual cycles, it is desirable to estimate their inter-annual variability. To this end, we compute for each month the standard deviation of the N_2O mixing ratio, M_y and A_z across the ten simulated years. Figures 7 and 8 show the annual cycles of these standard deviations for each dataset, at the same pressure level and latitude bands as in previous figures, and using the same color code. The polar regions (Fig. 8) are separated from the other latitude bands (Fig. 7) because they are characterized by much larger inter-annual variability for M_y and A_z.

We first consider the variability of the N_2O mixing ratio (Figs.7 and 8 top rows). The WACCM-CCMI simulations agree remarkably well with BRAM2, with the exception of the southern middle latitudes (Fig.7(a)). In the northern mid-latitudes (Fig.7(d)) the N_2O variability in WACCM-CCMI strongly depends on the considered realization. The CTM experiments generally underestimate the inter-annual variability of N_2O compared to BRAM2, with the exception of ERAI in the southern Tropics (Fig.7(b)). Figures 7(f) and 7(g) show the inter-annual variability of A_z in the northern and southern Tropics respectively. The datasets disagree more in these regions than in the other latitude bands, with WACCM-CCMI and JRA55 showing the smallest variabilities and BRAM2 and ERAI the largest. In the middle latitudes (Figs. 7(e) and 7(h)) A_z has the largest variability in winter and the summertime values are close to zero every year. In the antarctic region (Fig. 8(c)) the contribution of the upwelling to the N_2O abundances does not change much from year to year except in October during the vortex break-up, while in the arctic region (Fig. 8(d)) the wintertime inter-annual variability is larger.

https://doi.org/10.5194/acp-2020-262
Preprint. Discussion started: 16 April 2020


Atmospheric Chemistry and Physics Discussions

We now move to the variability of the horizontal mixing term M_y starting from the Tropics (Figs. 7(j) and 7(k)). In the southern tropics (Fig. 7(j)) M_y shows generally a small inter-annual variability with larger values in the second part of the year in the reanalyses but not in WACCM-CCMI. In the northern tropics (Fig. 7(k)) M_y is variable mostly from November until May with a very good agreement among the reanalyses, except in January when it is much more variable in BRAM2. The variability of M_y in the northern tropics is clearly underestimated in WACCM-CCMI. In the mid-latitudes the variability of M_y peaks in winter/spring in both hemispheres (Fig. 7(i) and (l)). WACCM-CCMI finds the same amount of variability in both hemispheres, while according to the reanalyses it is larger in the NH where the BRAM2 dataset is much more variable than all the others. In the antarctic region (Fig. 8(e)) M_y is highly variable in late winter and spring with a peak in October. All reanalyses agree, while in WACCM-CCMI the peak is reacheed one month earlier and the variability strongly depends on the model realization. The Arctic (Fig. 8(f)) is characterized by a very large wintertime variability of M_y. Among the reanalyses BRAM2 presenting the largest variability and MERRA the smallest. The variability with WACCM-CCMI is similar to the dynamical reanalyses and again depends on the model realization.

4 Discussion

We have described and compared the impact of the BDC on the N_2O rate of change in the chemical reanalysis BRAM2, three realizations and one sensitivty test with WACCM, and the BASCOE CTM driven by four different dynamical reanalyses. In summary, the present study reveals a good agreement at 15 hPa between WACCM-CCMI and BRAM2 in terms of the mid-stratospheric N_2O mixing ratio, while the CTM runs show a large spread (approximately 20%), especially in the Tropics (Figs. 5 and 6 top rows). The vertical advection term A_z agrees well across the datasets, except in the southern mid-latitudes and polar regions (Figs. 4 and 5 middle row). Large differences arise in the representation of M_y, in particular in the wintertime polar regions (Figs. 3 and 4). The inter-annual variability of the N_2O mixing ratio is in excellent agreement between WACCM-CCMI and BRAM2, while the CTM delivers overall smaller variabilities. We now discuss some possible causes of these results in light of the current literature about the modeling of the BDC.

4.1 Polar regions

It is interesting to highlight the differences between the wintertime North Pole and South Pole, because the hemispheric differences in wave activity (Scaife and James, 2000; Kidston et al., 2015) play a crucial role in the N_2O TEM budget. Above the Arctic in the middle stratosphere the N_2O abundances simulated by WACCM agree with the BRAM2 reanalysis and the advection term is also in good agreement (Fig. 6). This region is characterized by a very variable polar vortex with a shorter life span than the antarctic vortex (Randel and Newman, 1998; Waugh and Randel, 1999), resulting in an enhanced contribution of the horizontal mixing to the N_2O budget during winter compared to the Antarctic (Fig. 6(i)). Compared to the reanalyses, WACCM shows in this region a 2-fold underestimation of the N_2O changes due to horizontal mixing during winter; this can also be seen in the northern Tropics and middle latitudes (Fig. 6 bottom row). We consider that this disagreement between

https://doi.org/10.5194/acp-2020-262
Preprint. Discussion started: 16 April 2020


Atmospheric Chemistry and Physics Discussions

WACCM and the reanalyses is meaningful because the relative importance of the residual term is small in the NH. Note that WACCM is among the CCMI models with the lowest contribution of mixing to Age of Air (Fig. 2 in Dietmüller et al., 2018).

Above the Antarctic in the reanalyses, the relative importance of the residual is considerable (Figs. 4 and Fig. 5(g)) as it may cancel out most of the M_y contribution. Hence it is necessary to better understand its physical meaning. Dietmüller et al. (2017) applied the TEM continuity equation to the Age of Air (AoA). Computing the "resolved aging by mixing" (i.e. the AoA counterpart of $M_y + M_z$) as the time integral of the local mixing tendency along the residual circulation trajectories, and the "total aging by mixing" as the difference between the mean AoA and the residual circulation transit time, they defined the "aging by mixing on unresolved scales" (i.e. by diffusion) as the difference between the latter and the former. This "aging by diffusion", which can be related by construction to our residual term, arises around 60° S from the gradients due to the polar vortex edge. Even though we use a real tracer (N_2O) with a different TEM formulation, we find a qualitative agreement with this analysis based on AoA: our residual term is larger in regions characterized by strong gradients such as the Antarctic vortex edge, and larger with dynamics constrained to a reanalysis than with a free-running CCM (see EMAC results in Fig. 1d by Dietmüller et al., 2017). We propose to interpret the residual as the sum of mixing at unresolved scales and spurious numerical errors (Abalos et al., 2017).

Over the Antarctic Pole and below 30 hPa, M_y agrees remarkably well in all datasets during winter (Fig. 4). Closer to the vortex edge and above 30 hPa, the wintertime decrease of N_2O in the middle stratosphere is mainly due to vertical advection in WACCM-CCMI, while the reanalyses, especially BRAM2, show that the horizontal mixing also plays a major role (Fig. 5). The impact of horizontal mixing on N_2O inside the wintertime polar vortex in the reanalyses should not be surprising. de la Cámara et al. (2013) and Abalos et al. (2016a) showed, using observations and reanalyses respectively, that the isentropic mixing is not negligible inside the vortex. In constrast with the reanalyses, in WACCM-CCMI the M_y contribution is close to zero in the antarctic vortex and maximum along the vortex edge (Fig. 4). This disagreement can be related to differences in the zonal wind: it is overestimated above 30 km in subpolar latitudes (Garcia et al., 2017) and the polar jet is not tilted equatorward as in the reanalyses (Fig. 4). Yet, the differences in M_y and A_z above the Antarctic in winter should be put into perspective with the large residual term that points to an incomplete TEM budget (Figs. 4 right column and 5 left column). Near the Antarctic polar vortex, the assumptions of the TEM analysis (such as small amplitude waves) are less valid leading to larger errors in the evaluation of the mean transport and eddy fluxes (Miyazaki and Iwasaki, 2005).

During the SH spring the vortex breakup leads to an increased wave activity reaching the Antarctic (Randel and Newman, 1998), and mid-stratospheric M_y is in better agreement among all datasets and WACCM-CCMI exhibits a larger internal variability (Fig. 5(g)). Figure 5 also shows one realization of the earlier version WACCM4 which suffered from a larger cold bias above the Antarctic (see Sect. 2.1). In WACCM-CCMI, the parameterization of gravity waves was adjusted in order to reduce this issue while not significantly changing the dynamics in the NH. This results in an enhanced polar downwelling compared to WACCM4 (Garcia et al., 2017). Above the Antarctic the modification of the gravity waves in WACCM-CCMI results in a more realistic simulation of the N_2O mixing ratio in the austral spring compared to WACCM4 (Fig. 5(a)). While M_y does not show a significant impact of the gravity waves modification (Fig. 5(g)), A_z is stronger in WACCM-CCMI than in WACCM4 (Fig. 5(d)), this is evidently due to the stronger downwelling in WACCM-CCMI. Figure 9(a) shows the climatological mean of the

https://doi.org/10.5194/acp-2020-262
Preprint. Discussion started: 16 April 2020


Atmospheric Chemistry and Physics Discussions

monthly residual vertical velocities (see Eq. (3b)) at 15 hPa over the Antarctic. This comparison between the WACCM versions was already shown in Garcia et al. (2017, Fig. 10), we repeat it here adding the reanalyses. In November-December the weaker dowwelling in WACCM-CCMI agrees well with the reanalyses. Throughout the rest of the year WACCM-CCMI simulates a stronger downwelling than all reanalyses (also at lower levels, not shown). This difference raises the question whether the residual vertical velocity is correctly represented in WACCM-CCMI or in the dynamical reanalyses.

Above the Antarctic inter-annual variability of the vertical advection and the horizontal mixing terms is maximum during spring (Fig. 8), due to the large inter-annual variability in vortex breakup dates (Strahan et al., 2015). The lower wintertime variability would increase if a longer period was considered to include the exceptional Antarctic vortices of 2002 (Newman and Nash, 2005) and 2019 (Yamazaki et al., 2019). Above the Arctic the horizontal mixing and the vertical advection terms are most variable during winter, reflecting the frequent disruptions of the northern polar vortex by sudden stratospheric warmings (Butler et al., 2017).

4.2 Middle latitudes

In both hemispheres the residual term is smaller than in the polar regions, i.e. the TEM budget is well-closed. The location of the subtropical transport barriers (around 30° N and S) and the extension of the northern surf zone compare well between WACCM-CCMI and the reanalyses (Figs. 3 and 4). In the summertime lower stratosphere, we note N_2O increases due to horizontal mixing above the subtropical jets in both hemispheres and for all datasets (Figs. 3 and 4 middle columns). This behavior is consistent with early calculations of the effective diffusivity (Haynes and Shuckburgh, 2000b). It is due to transient Rossby waves that cannot travel further up into the stratosphere due to the presence of critical lines (Abalos et al., 2016b).

In the mid-stratospheric SH both A_z and M_y peak in mid-winter in the WACCM-CCMI simulations, while in the reanalyses these maxima are reached three months later (Fig. 5(e)). This is related to the earlier minimum in the downwelling velocity $\bar{w}^*$ simulated by WACCM-CCMI (Fig. 9(b)), that affects the vertical advection term A_z and, by compensation, the horizontal mixing term M_y (Fig. 5(h)). In the southern mid-latitudes the compensating contributions of A_z and M_y are stronger for JRA55 than for the other reanalyses (up to twice larger in September, see Fig. 5(e),(h)). This reflects the more intense BDC in JRA55 that resulted in the youngest mean AoA (mAoA) in the whole stratosphere (Chabrillat et al., 2018).

4.3 Tropics

In the tropical regions the CTM results show large differences in the N_2O mixing ratio depending on the input reanalysis (Figs. 5(c) and 6(a)). In regions where the mAoA is less than 4.5 years and N_2O is greater than 150 ppb, i.e. in the tropical regions and lower stratospheric middle latitudes (Strahan et al., 2011), the N_2O mixing ratio is inverserly proportional to the mAoA, because faster upwelling (younger air) implies more N_2O transported from lower levels, decreasing its residence time and resulting in a limited chemical destruction (Hall et al., 1999; Galytska et al., 2019). The dynamical reanalyses also produce large differences in mAoA at 15 hPa: MERRA delivers the oldest mAoA and MERRA2, ERAI and JRA55 progressively show younger mAoA (Fig. 4(b) in Chabrillat et al., 2018). Hence the large discrepancies in N_2O vmr can be explained by the large differences in mAoA, while M_y and A_z contribute to rates of change of N_2O.

https://doi.org/10.5194/acp-2020-262
Preprint. Discussion started: 16 April 2020


Atmospheric Chemistry and Physics Discussions

As in the middle latitudes, the TEM budget is well-closed in the tropical regions. The upwelling term A_z agrees very well in the reanalyses (Figs. 5(f) and 6(d)). This can be related to the good agreement in the tropical upwelling velocity at 15 hPa according to mAoA diagnostics (Fig. 4(d) in Chabrillat et al., 2018). In the southern tropics A_z has a pronounced annual cycle in the middle stratosphere that is not present in the northern tropics (Figs. 5(f) and 6(d)). As found previously with GEOSCCM (Tweedy et al., 2017), no such asymmetry can be seen in the lower stratosphere (not shown). With respect to inter-hemispheric differences in M_y, WACCM disagrees with the reanalyses: according to WACCM M_y has a larger impact in the southern tropics than in the northern tropics, but according to the reanalyses M_y has a much larger impact in the northern tropics (Figs. 5(i) and 6(g)).

In the Tropics the inter-annual variability of the N_2O mixing ratio depends considerably on the dataset (Figs. 7(b) and 7(c)). Among the CTM simulations, ERAI succeeds to deliver $\sigma(\bar{X})$ as large as BRAM2 and WACCM-CCMI in the southern tropics, but not in the northern tropics. The inter-annual variability of A_z (Figs. 7(f) and 7(g)) can be related to the impact of the QBO on the tropical upwelling (Flury et al., 2013). Among MERRA, ERAI and JRA55 the fraction of variance in deseasonalized tropical upwelling $\bar{w}^*$ that is associated with the QBO is the largest with ERAI (Abalos et al., 2015). Our findings support this conclusion since the largest $\sigma(\bar{A}_z)$ among the reanalyses is again found with ERAI (Fig. 7). A detailed analysis of the impact of the QBO on the BDC as illustated here goes beyond the scope of this study.

5 Summary and Conclusions

We have evaluated the climatological (2005-2014) N_2O transport processes in the stratosphere using the tracer continuity equation in the TEM formalism. In particular we considered the horizontal mixing and the vertical advection terms (M_y and A_z respectively). The upwelling term A_z reduces the N_2O concentrations in the Tropics and increases it in the extratropics, while M_y tends to reduce the meridional gradients of N_2O and presents large hemispheric differences. Since M_y or A_z contribute to the local and instantaneous rates of change of N_2O, this analysis is complementary to time-integrated diagnostics such as mAoA or the N_2O mixing ratio itself. The comparison investigates a variety of datasets, from a free-running chemistry-climate model to a reanalysis where dynamics and chemistry are both constrained. The former comprises three realizations of the CCMI REF-C1 experiment by WACCM, and the latter is the chemical reanalysis of Aura MLS driven by ERA-Interim: BRAM2. The intercomparison also includes the BASCOE CTM driven by four dynamical reanalyses: ERAI, JRA55, MERRA and MERRA2 in order to contribute to the S-RIP.

Considering the N_2O mixing ratio in the middle stratosphere, all datasets agree in the annual cycle, with the large spread in the N_2O abundances of the CTM experiments ($\sim 20\%$) reflecting the diversity of mAoA obtained with the same model (Chabrillat et al., 2018). The upwelling term A_z also agrees among the datasets, especially in the NH where WACCM follows closely the reanalyses. With respect to the horizontal mixing term M_y, in the NH WACCM simulates a weaker impact compared to the reanalyses. In the southern tropics and middle latitudes the wintertime M_y is stronger in WACCM than in the reanalyses. The differences in M_y become striking in the wintertime Antarctic, where the polar vortex has a major role. According to the reanalyses the horizontal mixing plays an important role in that region, but that is not found by WACCM and this large

https://doi.org/10.5194/acp-2020-262
Preprint. Discussion started: 16 April 2020


Atmospheric Chemistry and Physics Discussions

wintertime M_y in the reanalyses is challenged by a nearly as large residual term. It should be noted that the residual term also includes effects from mixing by diffusion. An additional WACCM run with different gravity waves in the SH is used as a sensitivity test. This test has small impact on the horizontal mixing term M_y, but significantly modifies the vertical advection term A_z and the N_2O mixing ratio in the Antarctic.

The inter-annual variability of the mid-stratospheric horizontal mixing term M_y is largest in the polar regions. In the Antarctic it is related to the vortex breakup during spring, while in the Arctic it is related to the very variable polar vortex in winter. The inter-annual variability of A_z is characterized by a large spread in the mid-stratospheric tropical regions where WACCM-CCMI and JRA55 deliver a smaller contribution than the other reanalyses. This variability reflects the impact of the QBO on the tropical upwelling (Abalos et al., 2015).

The application of the TEM framework to tracer transport with reanalyses suffers from a poor closure of the budget in the polar regions. We chose to analyse these regions nonetheless because the differences in M_y between WACCM and the reanalyses are larger than the residual term, but it remains important to better understand the causes of these large uncertainties. To this end, detailed studies of transport in the polar stratosphere are needed, e.g. comparing the residual circulations with indirect estimates derived from momentum and thermodynamic balances, and evaluating the effective diffusivity in each dataset (Abalos et al., 2015, 2016a).

The next step of this reasearch consists in the analysis of the inter-annual variations of the BDC, including the impact of the QBO and the El-Nino Southern Oscillation. Further extensions of this work would include the addition of new reanalysis products such as ERA5 and an intercomparison of several CCMs as already done for the residual circulation itself (Chrysanthou et al., 2019).

Data availability. The 9 monthly climatologies of the N_2O mixing ratios and TEM budget terms are freely available at the BIRA-IASB repository (http://repository.aeronomie.be) under https://doi.org/10.18758/71021057.

Author contributions. DM, SC and EM designed the study. YC provided support in installing and running the models. QE provided the chemical reanalysis BRAM2 and helped in its interpretation. MP ran the CTM experiments. DK provided the WACCM-CCMI realizations and helped in the interpretation of the WACCM datasets. DM wrote and ran the software tools to compute the TEM budgets and realized all the figures. DM, MA and SC analyzed the TEM budgets. DM and SC wrote the text. All co-authors contributed to the interpretation of the results and the reviews of the draft manuscripts.

Competing interests. The authors declare that thay have no conflict of interest.

https://doi.org/10.5194/acp-2020-262
Preprint. Discussion started: 16 April 2020

Atmospheric Chemistry and Physics Discussions

Acknowledgements. DM and MP are financially supported by the F.R.S. – FNRS (Brussels) through the ACCROSS research project (grant no. PDR.T.0040.16). EM is a research associate with the F.R.S. – FNRS. MA acknowledges funding from the Atracción de Talento Comunidad de Madrid grant 2016-T2/AMB-1405, and the Spanish National project STEADY (CGL2017-83198-R). We thank the reanalysis centers (ECMWF, NASA GSFC and JMA) for providing their support and data products. WACCM is a component of NCAR's CESM, which is supported by the NSF and the Office of Science of the US Department of Energy. The authors wish to acknowledge the contribution of Rolando Garcia in the discussion of the paper specifically for the model results of WACCM.

https://doi.org/10.5194/acp-2020-262
Preprint. Discussion started: 16 April 2020

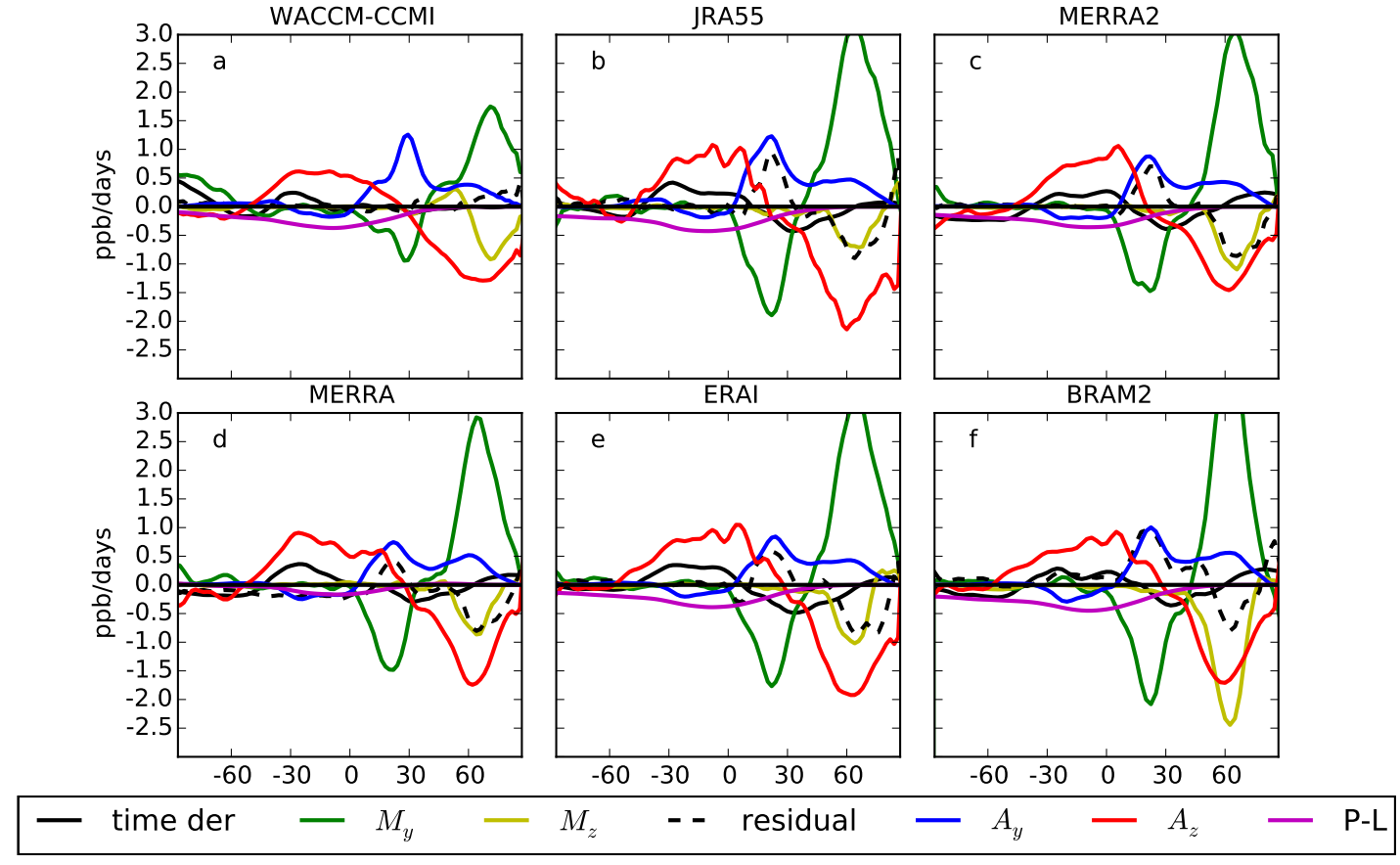

Figure 1. Latitudinal profiles of the N_2O TEM budget terms at 15 hPa averaged in DJF (2005-2014). Top row (left to right): WACCM-CCMI (a), JRA55 (b) and MERRA2 (c); bottom row (left to right): MERRA (d), ERAI (e) and BRAM2 (f). The color code is shown in the legend. Units are ppbv day^{-1}

https://doi.org/10.5194/acp-2020-262
Preprint. Discussion started: 16 April 2020

Atmospheric Chemistry and Physics Discussions

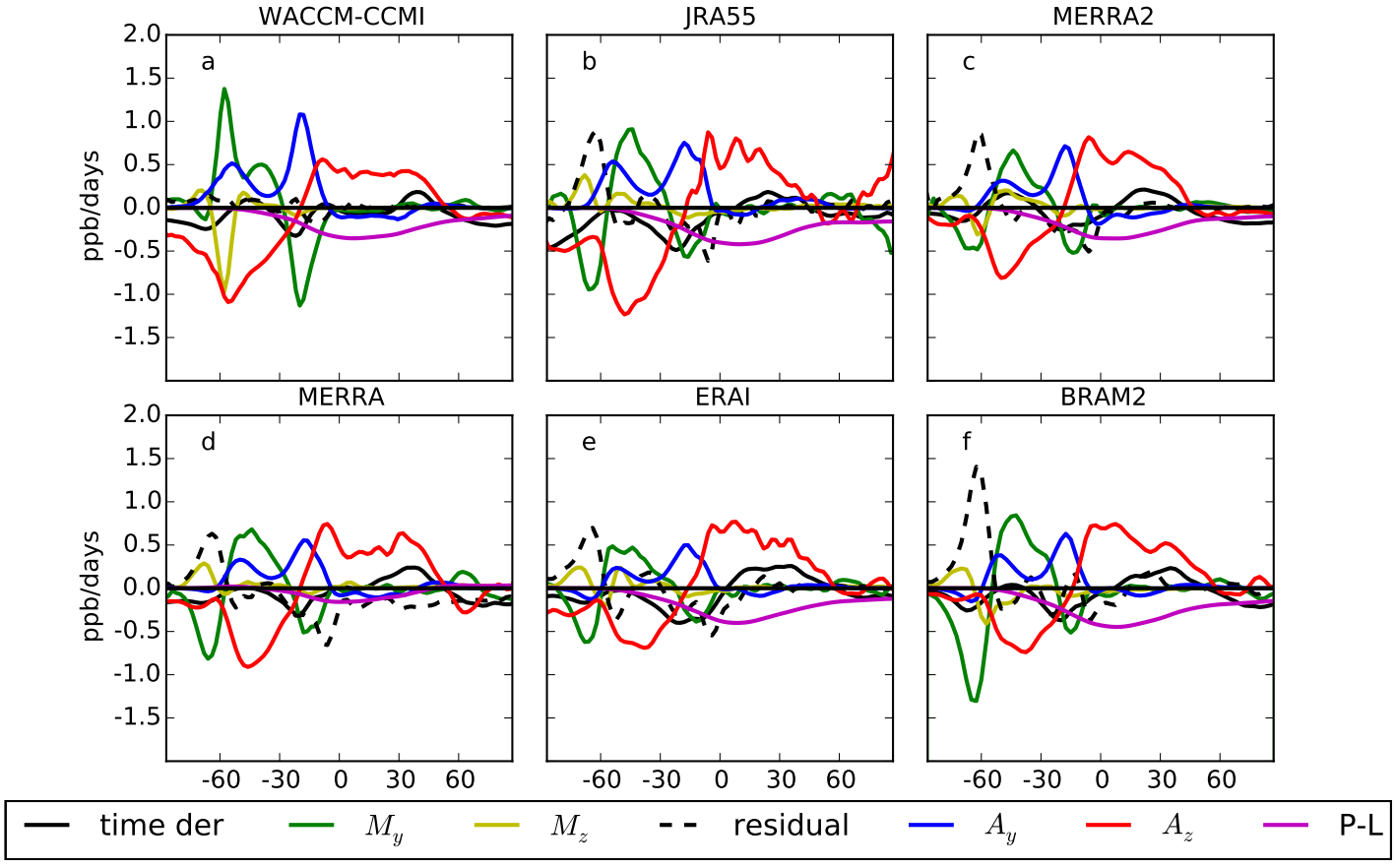

Figure 2. Same as previous figure but for JJA.

https://doi.org/10.5194/acp-2020-262
Preprint. Discussion started: 16 April 2020

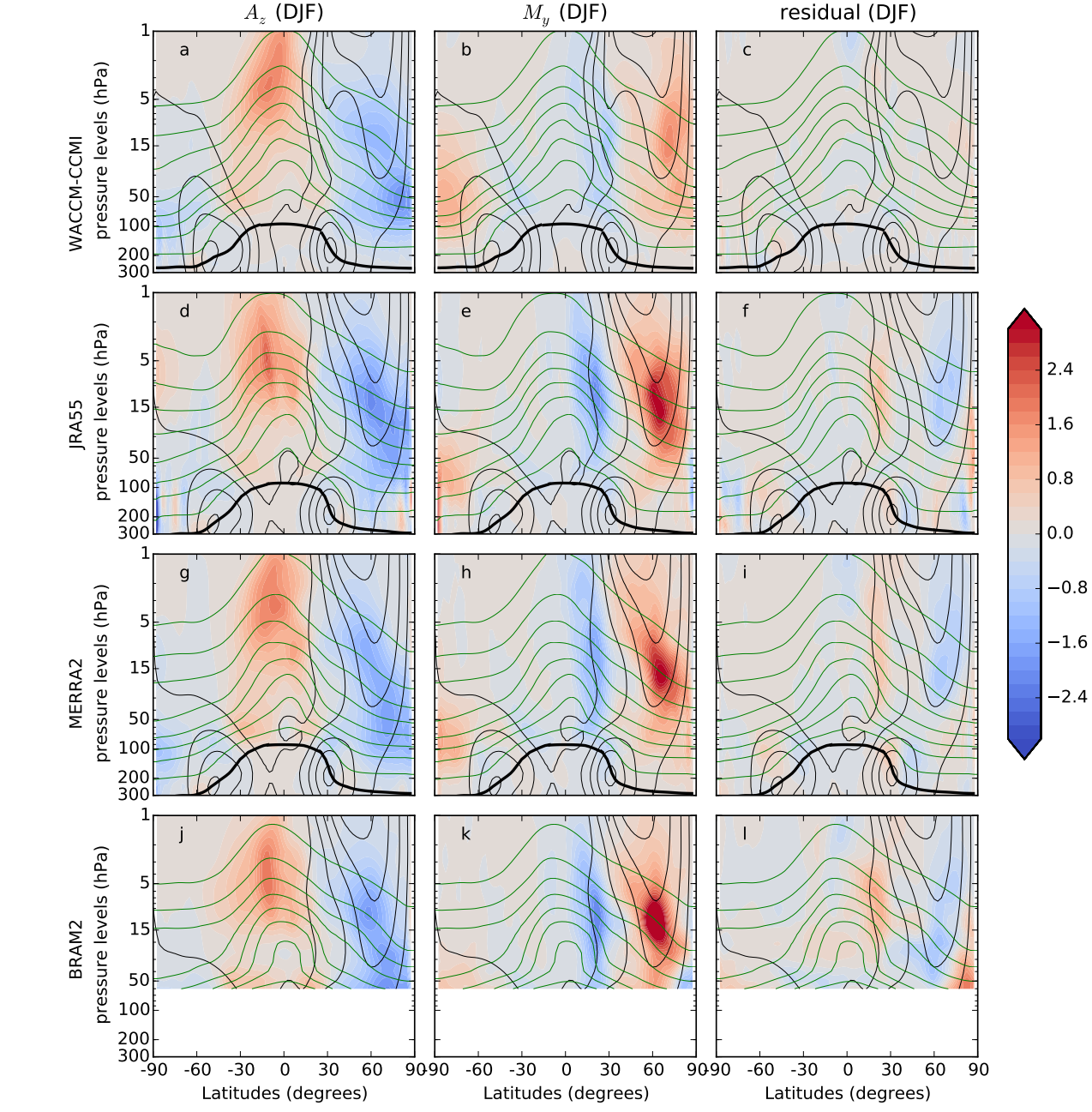

Figure 3. Climatological (2005-2014) latitude-pressure cross sections of three N_2O TEM budget terms averaged in DJF ($ppbv\,day^{-1}$): horizontal mixing term (left column), vertical residual advection term (central column) and residual term (right column). The datasets are, from top to bottom: WACCM-CCMI, JRA55, MERRA2, and BRAM2. The residual term for WACCM-CCMI is from a single realization of the model. The thin black lines show the zonal mean zonal wind (from 0 to 40 m/s every 10 m/s), the black thick line represents the dynamical tropopause for the considered season and the green thin lines show the climatological mixing ratio of N_2O (from 20 to 300 ppbv with 40 ppbv spacing).

https://doi.org/10.5194/acp-2020-262
Preprint. Discussion started: 16 April 2020

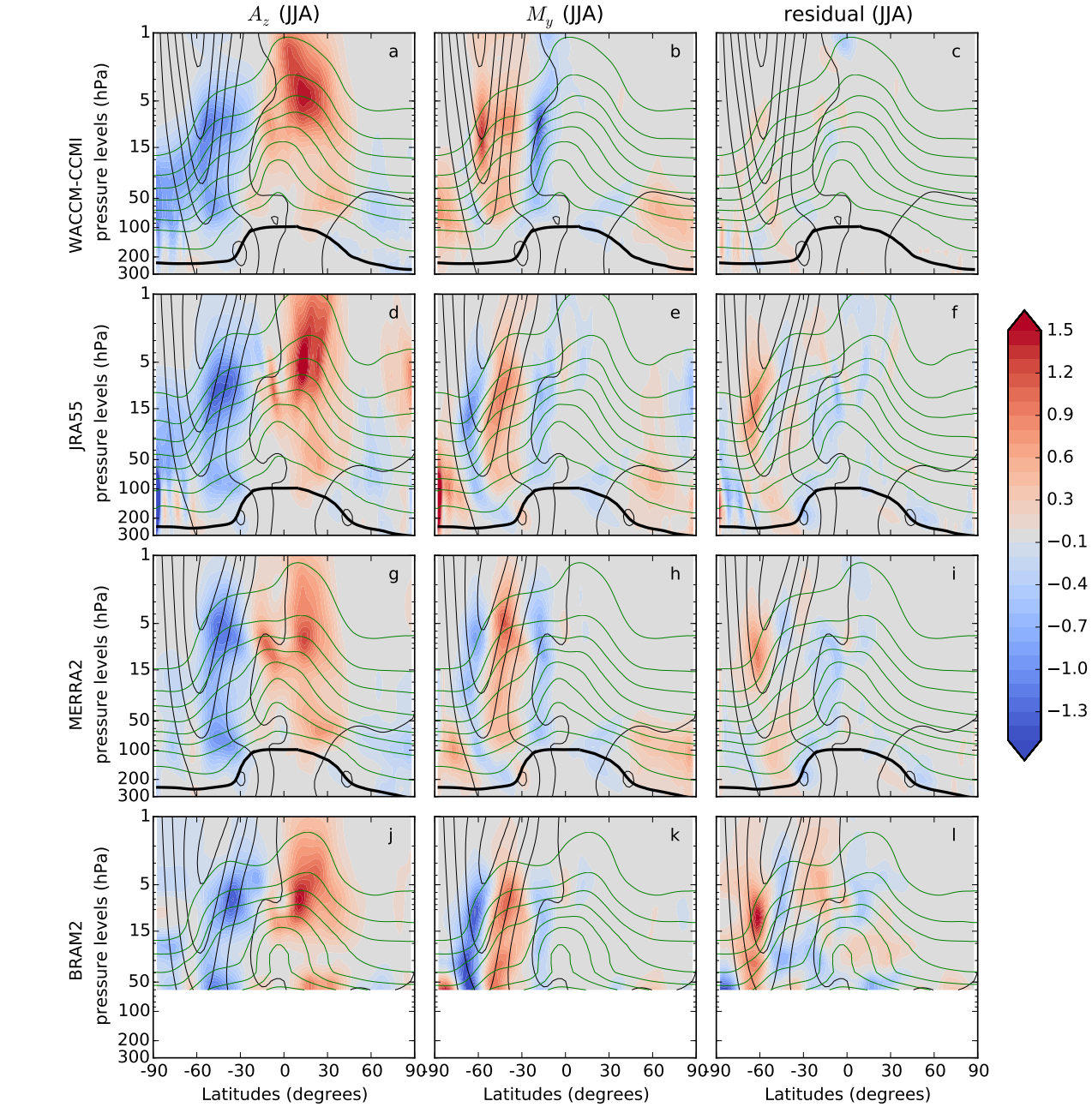

Figure 4. Same as previous figure but for JJA and with a different color scale. The thin black contours show the zonal mean zonal wind (from 0 to 100 m/s every 20 m/s).

https://doi.org/10.5194/acp-2020-262
Preprint. Discussion started: 16 April 2020

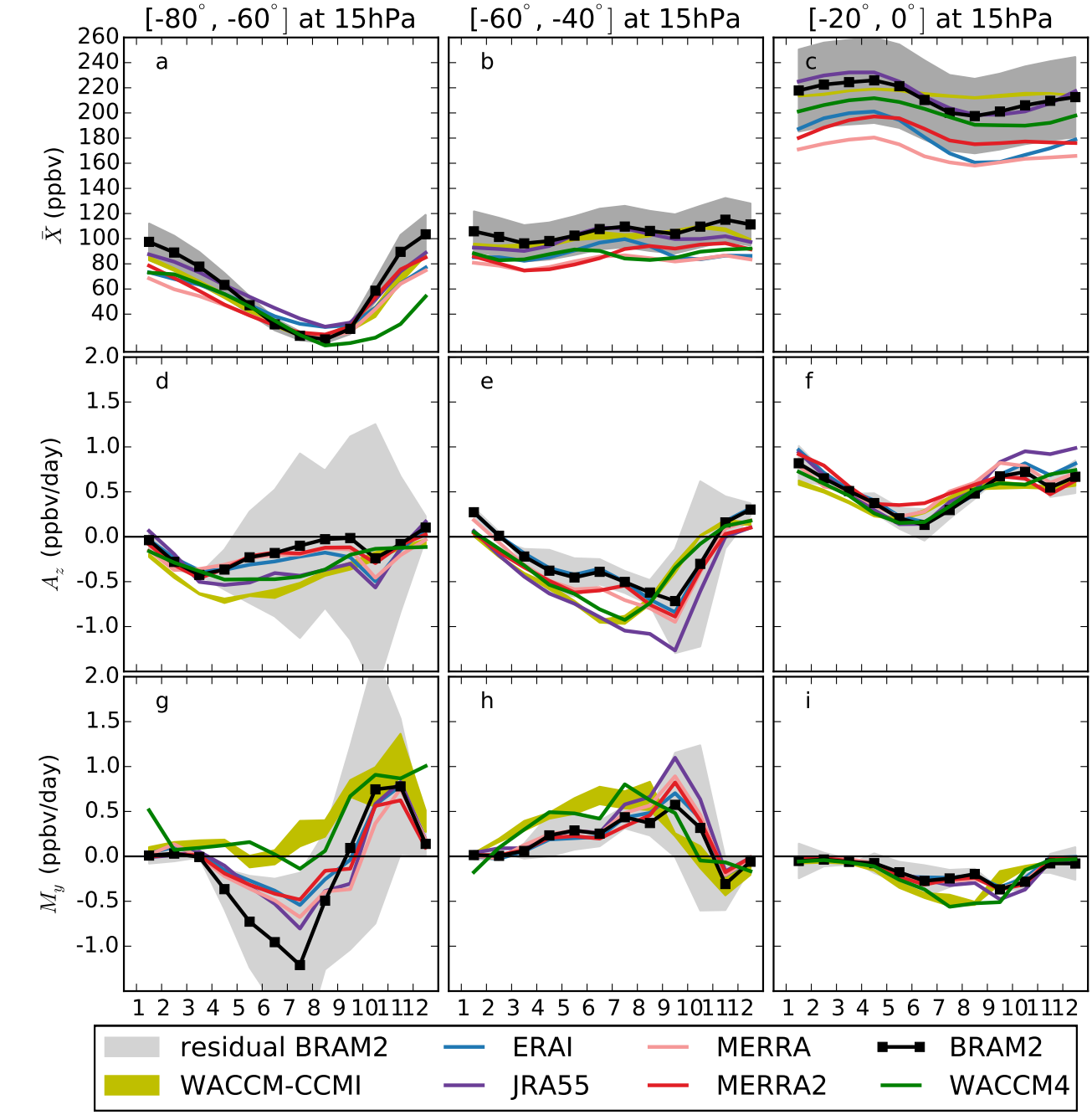

Figure 5. Monthly mean annual cycles at 15 hPa in the SH. First row: N_2O volume mixing ratio [ppbv], second row: horizontal mixing term [ppbv day^{-1}]; third row: vertical residual advection term [ppbv day^{-1}]. Left column: polar region (60°-80° S), middle column: mid-latitudes (40°-60° S), right column: Tropics (0°-20° S). The color code is shown in the legend. The olive envelope shows the 3 realizations of the WACCM-CCMI simulation. The dark grey shading (top row) shows 15% uncertainty around BRAM2. The light grey shading (middle and bottom rows) shows BRAM2 plus and minus the residual term.

https://doi.org/10.5194/acp-2020-262
Preprint. Discussion started: 16 April 2020

Atmospheric Chemistry and Physics Discussions

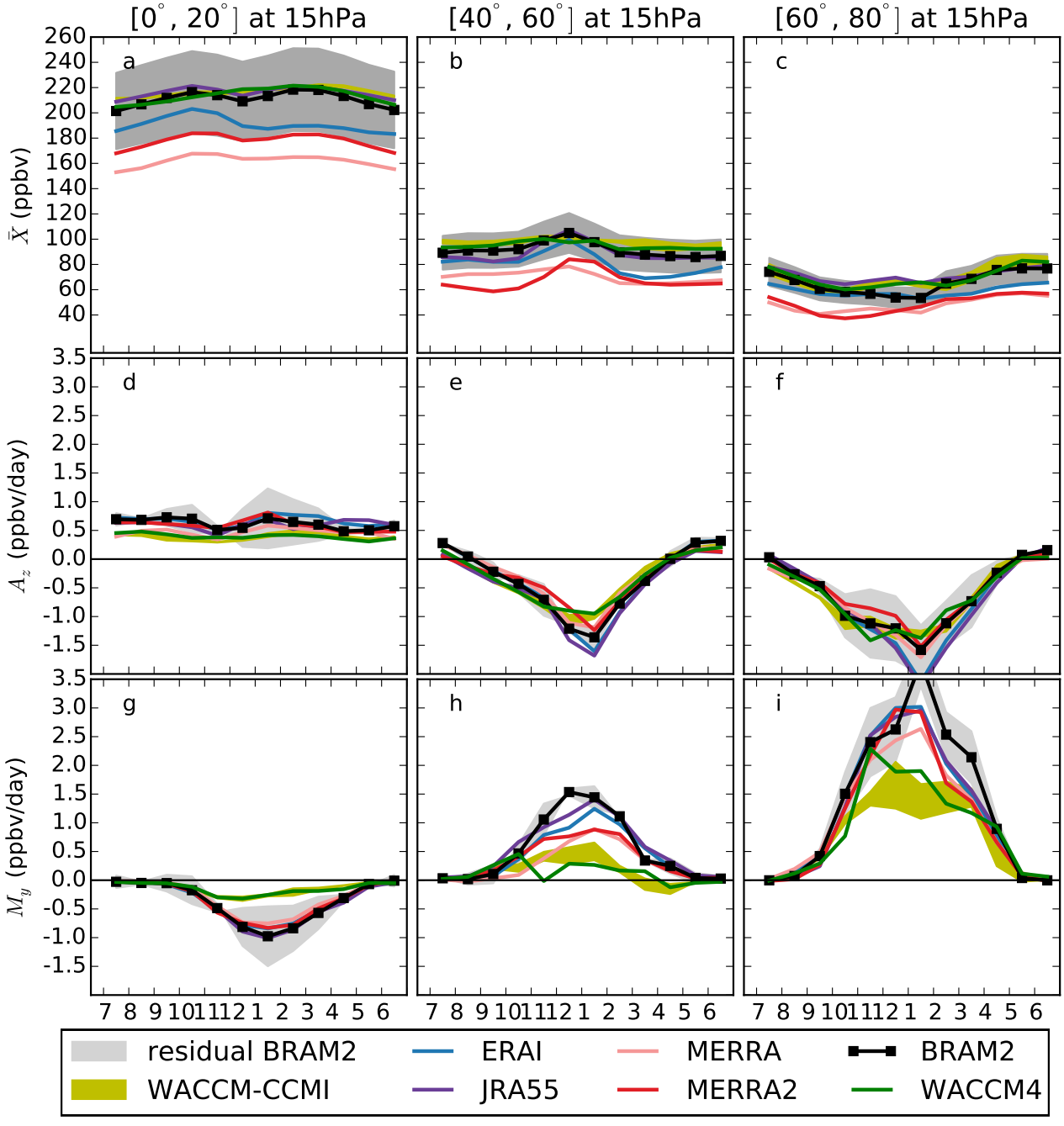

Figure 6. Same as previous figure but showing the NH.

https://doi.org/10.5194/acp-2020-262
Preprint. Discussion started: 16 April 2020

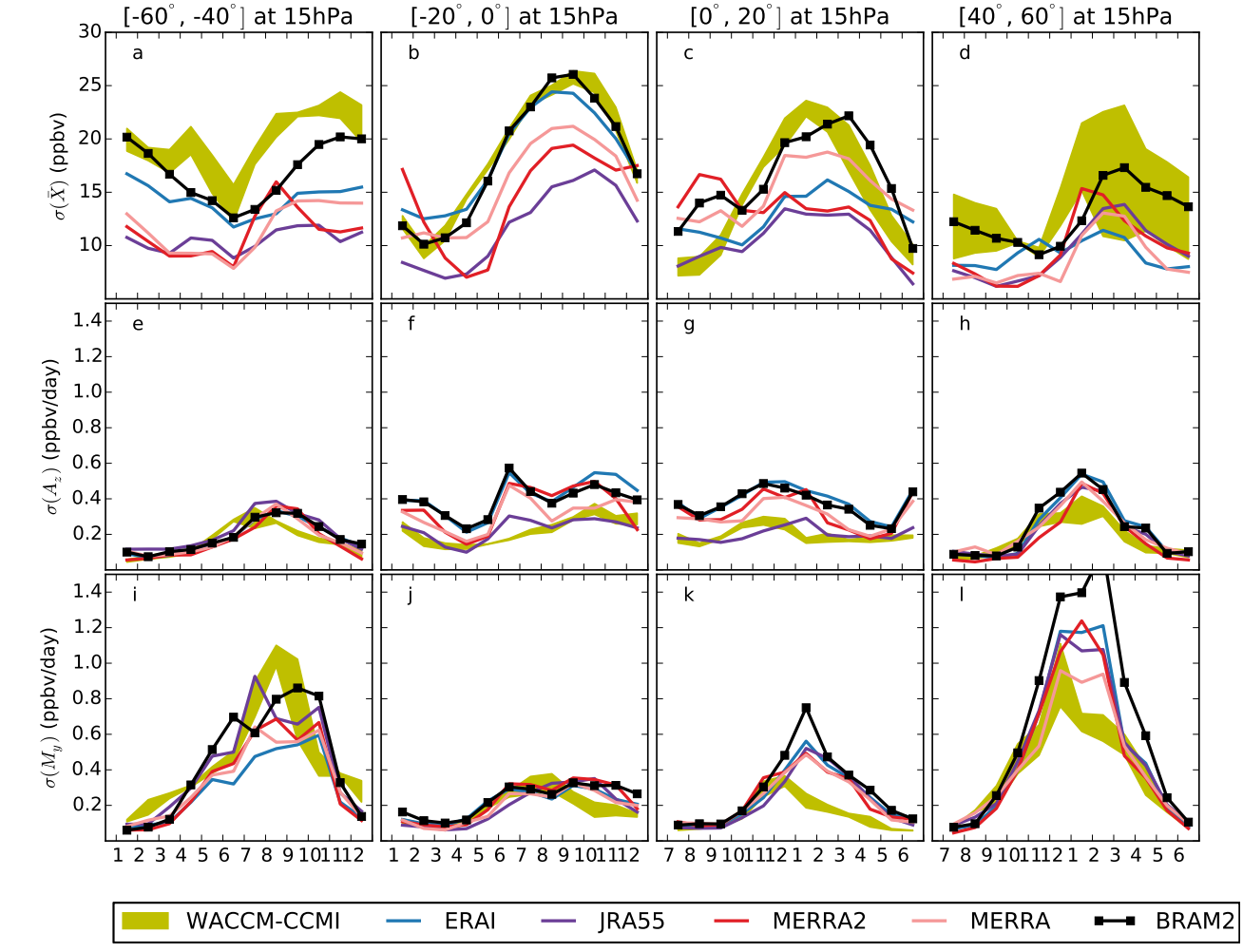

Figure 7. Monthly standard deviation over 2005-2014 at 15 hPa. First row: N_2O volume mixing ratio [ppb], second row: horizontal mixing term [ppbv day^{-1}]; third row: vertical residual advection term [ppbv day^{-1}]. From left to right: southern mid-latitudes (40°-60° S), southern tropics (0°-20° S), northern tropics (0°-20° N), northern mid-latitudes (40°-60° N). The color code is shown in the legend. The yellow envelope shows the 3 realizations of the WACCM-CCMI simulation.

https://doi.org/10.5194/acp-2020-262
Preprint. Discussion started: 16 April 2020

Atmospheric Chemistry and Physics Discussions

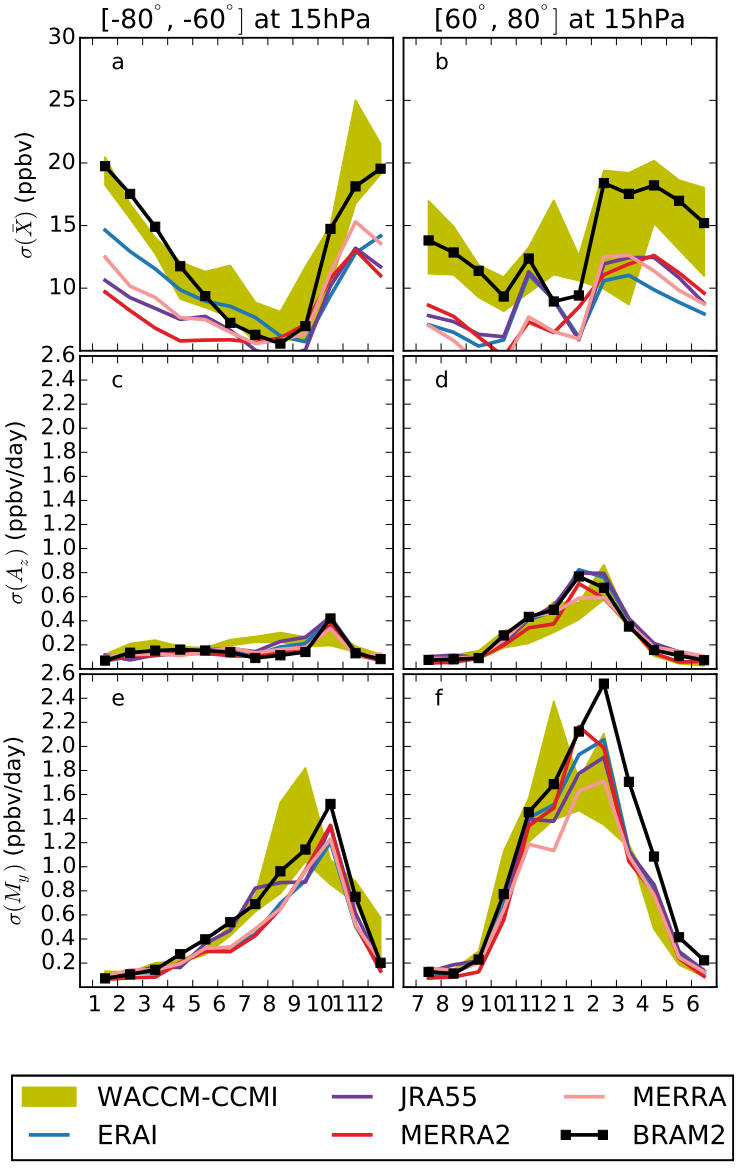

Figure 8. Same as previous figure but for the polar regions (left column: antarctic region, 80°-60° S; right column: arctic region, 60°-80° N).

https://doi.org/10.5194/acp-2020-262
Preprint. Discussion started: 16 April 2020

Atmospheric Chemistry and Physics Discussions

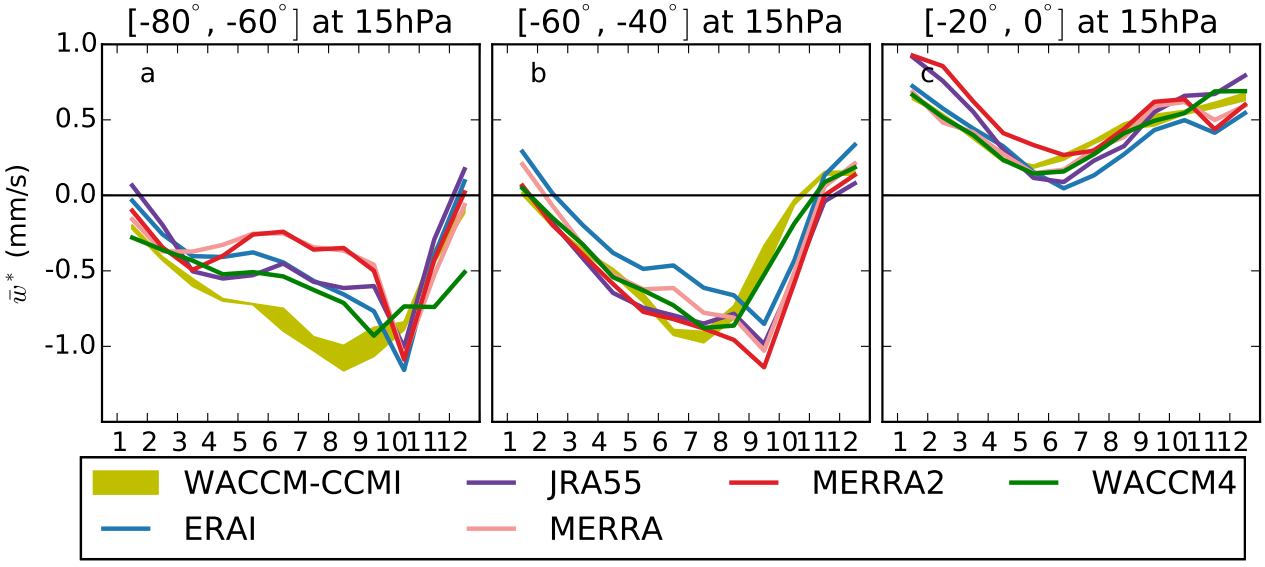

Figure 9. Monthly mean annual cycle of $\bar{w}^*$ at 15 hPa in the SH [$\mathrm{mm\,s^{-1}}$]. From left to right: southern mid-latitudes (40°-60° S), southern tropics (0°-20° S), northern tropics (0°-20° N), northern mid-latitudes (40°-60° N). The color code is shown in the legend. The yellow envelope shows the 3 realizations of the WACCM-CCMI simulation.

https://doi.org/10.5194/acp-2020-262
Preprint. Discussion started: 16 April 2020

Atmospheric Chemistry and Physics Discussions

References

Abalos, M., Randel, W., Kinnison, D., and Serrano, E.: Quantifying tracer transport in the tropical lower stratosphere using WACCM, Atmos. Chem. Phys, 13, 591–10, 2013.

Abalos, M., Legras, B., Ploeger, F., and Randel, W. J.: Evaluating the advective Brewer-Dobson circulation in three reanalyses for the period 1979–2012, Journal of Geophysical Research: Atmospheres, 120, 7534–7554, 2015.

Abalos, M., Legras, B., and Shuckburgh, E.: Interannual variability in effective diffusivity in the upper troposphere/lower stratosphere from reanalysis data, Quarterly Journal of the Royal Meteorological Society, 142, 1847–1861, 2016a.

Abalos, M., Randel, W. J., and Birner, T.: Phase-speed spectra of eddy tracer fluxes linked to isentropic stirring and mixing in the upper troposphere and lower stratosphere, Journal of the Atmospheric Sciences, 73, 4711–4730, 2016b.

Abalos, M., Randel, W. J., Kinnison, D. E., and Garcia, R. R.: Using the artificial tracer e90 to examine present and future UTLS tracer transport in WACCM, Journal of the Atmospheric Sciences, 74, 3383–3403, 2017.

Andrews, D. G., Holton, J. R., and Leovy, C. B.: Middle atmosphere dynamics, 40, Academic press, 1987.

Baldwin, M., Gray, L., Dunkerton, T., Hamilton, K., Haynes, P., Randel, W., Holton, J., Alexander, M., Hirota, I., Horinouchi, T., et al.: The quasi-biennial oscillation, Reviews of Geophysics, 39, 179–229, 2001.

Birner, T. and Bönisch, H.: Residual circulation trajectories and transit times into the extratropical lowermost stratosphere, Atmospheric Chemistry and Physics, 11, 817–827, https://doi.org/10.5194/acp-11-817-2011, https://www.atmos-chem-phys.net/11/817/2011/, 2011.

Brasseur, G. P. and Solomon, S.: Aeronomy of the middle atmosphere: chemistry and physics of the stratosphere and mesosphere, vol. 32, Springer Science & Business Media, 2006.

Brewer, A.: Evidence for a world circulation provided by the measurements of helium and water vapour distribution in the stratosphere, Quarterly Journal of the Royal Meteorological Society, 75, 351–363, 1949.

Butchart, N.: The Brewer-Dobson circulation, Reviews of geophysics, 52, 157–184, 2014.

Butchart, N., Cionni, I., Eyring, V., Shepherd, T., Waugh, D., Akiyoshi, H., Austin, J., Brühl, C., Chipperfield, M., Cordero, E., et al.: Chemistry–climate model simulations of twenty-first century stratospheric climate and circulation changes, Journal of Climate, 23, 5349–5374, 2010.

Butler, A. H., Sjoberg, J. P., Seidel, D. J., and Rosenlof, K. H.: A sudden stratospheric warming compendium., Earth System Science Data, 9, 2017.

Cameron, C., Bodeker, G. E., Conway, J. P., Stuart, S., and Renwick, J.: Simulating the Antarctic stratospheric vortex transport barrier: comparing the Unified Model to reanalysis, Climate Dynamics, pp. 1–12, 2019.

Chabrillat, S., Vigouroux, C., Christophe, Y., Engel, A., Errera, Q., Minganti, D., Monge-Sanz, B. M., Segers, A., and Mahieu, E.: Comparison of mean age of air in five reanalyses using the BASCOE transport model, Atmospheric Chemistry and Physics, 18, 14 715–14 735, 2018.

Charney, J. G. and Drazin, P. G.: Propagation of planetary-scale disturbances from the lower into the upper atmosphere, Journal of Geophysical Research, 66, 83–109, 1961.

Chrysanthou, A., Maycock, A. C., Chipperfield, M. P., Dhomse, S., Garny, H., Kinnison, D., Akiyoshi, H., Deushi, M., Garcia, R. R., Jöckel, P., Kirner, O., Pitari, G., Plummer, D. A., Revell, L., Rozanov, E., Stenke, A., Tanaka, T. Y., Visioni, D., and Yamashita, Y.: The effect of atmospheric nudging on the stratospheric residual circulation in chemistry–climate models, Atmospheric Chemistry and Physics, 19, 11 559–11 586, https://doi.org/10.5194/acp-19-11559-2019, https://www.atmos-chem-phys.net/19/11559/2019/, 2019.

https://doi.org/10.5194/acp-2020-262
Preprint. Discussion started: 16 April 2020

Atmospheric Chemistry and Physics Discussions

Conley, A. J., Garcia, R., Kinnison, D., Lamarque, J.-F., Marsh, D., Mills, M., Smith, A. K., Tilmes, S., Vitt, F., Morrison, H., et al.: Description of the NCAR community atmosphere model (CAM 5.0), NCAR technical note, 2012.

Davis, S. M., Rosenlof, K. H., Hassler, B., Hurst, D. F., Read, W. G., Vömel, H., Selkirk, H., Fujiwara, M., and Damadeo, R.: The Stratospheric Water and Ozone Satellite Homogenized (SWOOSH) database: A long-term database for climate studies, Earth system science data, 8, 461, 2016.

de la Cámara, A., Mechoso, C. R., Mancho, A. M., Serrano, E., and Ide, K.: Isentropic Transport within the Antarctic Polar-Night Vortex: Rossby Wave Breaking Evidence and Lagrangian Structures, Journal of the Atmospheric Sciences, 70, 2982–3001, https://doi.org/10.1175/JAS-D-12-0274.1, 2013.

Dee, D. P., Uppala, S., Simmons, A., Berrisford, P., Poli, P., Kobayashi, S., Andrae, U., Balmaseda, M., Balsamo, G., Bauer, d. P., et al.: The ERA-Interim reanalysis: Configuration and performance of the data assimilation system, Quarterly Journal of the royal meteorological society, 137, 553–597, 2011.

Dietmüller, S., Garny, H., Plöger, F., Jöckel, P., and Cai, D.: Effects of mixing on resolved and unresolved scales on stratospheric age of air, Atmospheric Chemistry and Physics, 17, 7703, 2017.

Dietmüller, S., Eichinger, R., Garny, H., Birner, T., Boenisch, H., Pitari, G., Mancini, E., Visioni, D., Stenke, A., Revell, L., et al.: Quantifying the effect of mixing on the mean age of air in CCMVal-2 and CCMI-1 models, Atmospheric Chemistry and Physics, 18, 6699–6720, 2018.

Dobson, G. M. B.: Origin and distribution of the polyatomic molecules in the atmosphere, Proceedings of the Royal Society of London. Series A. Mathematical and Physical Sciences, 236, 187–193, 1956.

Dobson, G. M. B., Harrison, D., and Lawrence, J.: Measurements of the amount of ozone in the Earth2̌019s atmosphere and its relation to other geophysical conditions.2̌014Part III, Proceedings of the Royal Society of London. Series A, Containing Papers of a Mathematical and Physical Character, 122, 456–486, 1929.

Eichinger, R., Dietmüller, S., Garny, H., Šácha, P., Birner, T., Bönisch, H., Pitari, G., Visioni, D., Stenke, A., Rozanov, E., et al.: The influence of mixing on the stratospheric age of air changes in the 21st century, Atmospheric Chemistry and Physics, 19, 921–940, 2019.

Engel, A., Möbius, T., Bönisch, H., Schmidt, U., Heinz, R., Levin, I., Atlas, E., Aoki, S., Nakazawa, T., Sugawara, S., et al.: Age of stratospheric air unchanged within uncertainties over the past 30 years, Nature Geoscience, 2, 28, 2009.

Engel, A., Bönisch, H., Ullrich, M., Sitals, R., Membrive, O., Danis, F., and Crevoisier, C.: Mean age of stratospheric air derived from AirCore observations, Atmospheric Chemistry and Physics, 17, 6825–6838, 2017.

Errera, Q., Chabrillat, S., Christophe, Y., Debosscher, J., Hubert, D., Lahoz, W., Santee, M. L., Shiotani, M., Skachko, S., von Clarmann, T., and Walker, K.: Technical note: Reanalysis of Aura MLS Chemical Observations, Atmospheric Chemistry and Physics Discussions, 2019, 1–60, https://doi.org/10.5194/acp-2019-530, https://www.atmos-chem-phys-discuss.net/acp-2019-530/, 2019.

Flury, T., Wu, D. L., and Read, W.: Variability in the speed of the Brewer–Dobson circulation as observed by Aura/MLS, Atmospheric Chemistry and Physics, 13, 4563–4575, 2013.

Froidevaux, L., Kinnison, D. E., Wang, R., Anderson, J., and Fuller, R. A.: Evaluation of CESM1 (WACCM) free-running and specified dynamics atmospheric composition simulations using global multispecies satellite data records, Atmospheric Chemistry and Physics, 19, 4783–4821, 2019.

Fujiwara, M., Wright, J. S., Manney, G. L., Gray, L. J., Anstey, J., Birner, T., Davis, S., Gerber, E. P., Harvey, V. L., Hegglin, M. I., et al.: Introduction to the SPARC Reanalysis Intercomparison Project (S-RIP) and overview of the reanalysis systems, Atmospheric Chemistry and Physics, 17, 1417–1452, 2017.

https://doi.org/10.5194/acp-2020-262
Preprint. Discussion started: 16 April 2020


Atmospheric Chemistry and Physics Discussions

Galytska, E., Rozanov, A., Chipperfield, M. P., Dhomse, Weber, M., Arosio, C., Feng, W., and Burrows, J. P.: Dynamically controlled ozone decline in the tropical mid-stratosphere observed by SCIAMACHY, Atmospheric Chemistry and Physics, 19, 767–783, https://doi.org/10.5194/acp-19-767-2019, https://www.atmos-chem-phys.net/19/767/2019/, 2019.

Garcia, R. R., Randel, W. J., and Kinnison, D. E.: On the determination of age of air trends from atmospheric trace species, Journal of the Atmospheric Sciences, 68, 139–154, 2011.

Garcia, R. R., Smith, A. K., Kinnison, D. E., Cámara, Á. d. l., and Murphy, D. J.: Modification of the gravity wave parameterization in the Whole Atmosphere Community Climate Model: Motivation and results, Journal of the Atmospheric Sciences, 74, 275–291, 2017.

Garfinkel, C. I., Aquila, V., Waugh, D. W., and Oman, L. D.: Time-varying changes in the simulated structure of the Brewer–Dobson Circulation, Atmospheric Chemistry and Physics, 17, 1313–1327, 2017.

Garny, H., Birner, T., Bönisch, H., and Bunzel, F.: The effects of mixing on age of air, Journal of Geophysical Research: Atmospheres, 119, 7015–7034, 2014.

Gelaro, R., McCarty, W., Suárez, M. J., Todling, R., Molod, A., Takacs, L., Randles, C. A., Darmenov, A., Bosilovich, M. G., Reichle, R., et al.: The modern-era retrospective analysis for research and applications, version 2 (MERRA-2), Journal of Climate, 30, 5419–5454, 2017.

Haenel, F., Stiller, G., Von Clarmann, T., Funke, B., Eckert, E., Glatthor, N., Grabowski, U., Kellmann, S., Kiefer, M., Linden, A., et al.: Reassessment of MIPAS age of air trends and variability, Atmospheric Chemistry and Physics, 15, 13 161–13 176, 2015.

Hall, T. M., Waugh, D. W., Boering, K. A., and Plumb, R. A.: Evaluation of transport in stratospheric models, Journal of Geophysical Research: Atmospheres, 104, 18 815–18 839, 1999.

Hardiman, S. C., Butchart, N., and Calvo, N.: The morphology of the Brewer–Dobson circulation and its response to climate change in CMIP5 simulations, Quarterly Journal of the Royal Meteorological Society, 140, 1958–1965, 2014.

Hardiman, S. C., Lin, P., Scaife, A. A., Dunstone, N. J., and Ren, H.-L.: The influence of dynamical variability on the observed Brewer-Dobson circulation trend, Geophysical Research Letters, 44, 2885–2892, 2017.

Haynes, P. and Shuckburgh, E.: Effective diffusivity as a diagnostic of atmospheric transport: 1. Stratosphere, Journal of Geophysical Research: Atmospheres, 105, 22 777–22 794, 2000a.

Haynes, P. and Shuckburgh, E.: Effective diffusivity as a diagnostic of atmospheric transport: 2. Troposphere and lower stratosphere, Journal of Geophysical Research: Atmospheres, 105, 22 795–22 810, 2000b.

Hegglin, M., Plummer, D., Shepherd, T., Scinocca, J., Anderson, J., Froidevaux, L., Funke, B., Hurst, D., Rozanov, A., Urban, J., et al.: Vertical structure of stratospheric water vapour trends derived from merged satellite data, Nature geoscience, 7, 768, 2014.

Holton, J.: An Introduction to Dynamic Meteorology, no. v. 1 in An Introduction to Dynamic Meteorology, Elsevier Science, https://books.google.be/books?id=fhW5oDv3EPsC, 2004.

Hurrell, J. W., Holland, M. M., Gent, P. R., Ghan, S., Kay, J. E., Kushner, P. J., Lamarque, J.-F., Large, W. G., Lawrence, D., Lindsay, K., et al.: The community earth system model: a framework for collaborative research, Bulletin of the American Meteorological Society, 94, 1339–1360, 2013.

Inness, A., Baier, F., Benedetti, A., Bouarar, I., Chabrillat, S., Clark, H., Clerbaux, C., Coheur, P., Engelen, R., Errera, Q., et al.: The MACC reanalysis: an 8 yr data set of atmospheric composition, Atmospheric chemistry and physics, 13, 4073–4109, 2013.

Kidston, J., Scaife, A. A., Hardiman, S. C., Mitchell, D. M., Butchart, N., Baldwin, M. P., and Gray, L. J.: Stratospheric influence on tropospheric jet streams, storm tracks and surface weather, Nature Geoscience, 8, 433, 2015.

https://doi.org/10.5194/acp-2020-262
Preprint. Discussion started: 16 April 2020

Atmospheric Chemistry and Physics Discussions

Kinnison, D., Brasseur, G., Walters, S., Garcia, R., Marsh, D., Sassi, F., Harvey, V., Randall, C., Emmons, L., Lamarque, J.-F., et al.: Sensitivity of chemical tracers to meteorological parameters in the MOZART-3 chemical transport model, Journal of Geophysical Research: Atmospheres, 112, 2007.

Kobayashi, S., Ota, Y., Harada, Y., Ebita, A., Moriya, M., Onoda, H., Onogi, K., Kamahori, H., Kobayashi, C., Endo, H., et al.: The JRA-55 reanalysis: General specifications and basic characteristics, Journal of the Meteorological Society of Japan. Ser. II, 93, 5–48, 2015.

Lean, J., Rottman, G., Harder, J., and Kopp, G.: SORCE contributions to new understanding of global change and solar variability, in: The Solar Radiation and Climate Experiment (SORCE), pp. 27–53, Springer, 2005.

Lin, S.-J.: A ̆201cvertically Lagrangian̆201d finite-volume dynamical core for global models, Monthly Weather Review, 132, 2293–2307, 2004.

Lin, S.-J. and Rood, R. B.: Multidimensional flux-form semi-Lagrangian transport schemes, Monthly Weather Review, 124, 2046–2070, 1996.

Livesey, NJ, e. a.: Long-term drifts in the 190 GHz measurements from the Aura Microwave Limb Sounder: Observations, insights, plans and guidance for data users, in preparation.

Livesey, N., Read, W., Wagner, P., Froidevaux, L., Lambert, A., Manney, G., Pumphrey, H., Santee, M., Schwartz, M., Wang, S., et al.: Earth Observing System (EOS) Aura Microwave Limb Sounder (MLS) version 4.2 x level 2 data quality and description document, JPL D-33509 rev. A, A, JPL publication, Pasadena, CA, USA, 2015.

Mahieu, E., Chipperfield, M., Notholt, J., Reddmann, T., Anderson, J., Bernath, P., Blumenstock, T., Coffey, M., Dhomse, S., Feng, W., et al.: Recent Northern Hemisphere stratospheric HCl increase due to atmospheric circulation changes, Nature, 515, 104, 2014.

Manney, G. L., Sabutis, J. L., Pawson, S., Santee, M. L., Naujokat, B., Swinbank, R., Gelman, M. E., and Ebisuzaki, W.: Lower stratospheric temperature differences between meteorological analyses in two cold Arctic winters and their impact on polar processing studies, Journal of Geophysical Research: Atmospheres, 108, 2003.

Marsh, D. R., Mills, M. J., Kinnison, D. E., Lamarque, J.-F., Calvo, N., and Polvani, L. M.: Climate change from 1850 to 2005 simulated in CESM1 (WACCM), Journal of climate, 26, 7372–7391, 2013.

Matthes, K., Marsh, D. R., Garcia, R. R., Kinnison, D. E., Sassi, F., and Walters, S.: Role of the QBO in modulating the influence of the 11 year solar cycle on the atmosphere using constant forcings, Journal of Geophysical Research: Atmospheres, 115, 2010.

McIntyre, M. E. and Palmer, T.: Breaking planetary waves in the stratosphere, Nature, 305, 593, 1983.

Miyazaki, K. and Iwasaki, T.: Diagnosis of meridional ozone transport based on mass-weighted isentropic zonal means, Journal of the atmospheric sciences, 62, 1192–1208, 2005.

Morgenstern, O., Hegglin, M. I., Rozanov, E., O'Connor, F. M., Abraham, N. L., Akiyoshi, H., Archibald, A. T., Bekki, S., Butchart, N., Chipperfield, M. P., et al.: Review of the global models used within phase 1 of the Chemistry-Climate Model Initiative (CCMI), Geoscientific Model Development, 2017.

Neale, R. B., Richter, J., Park, S., Lauritzen, P. H., Vavrus, S. J., Rasch, P. J., and Zhang, M.: The mean climate of the Community Atmosphere Model (CAM4) in forced SST and fully coupled experiments, Journal of Climate, 26, 5150–5168, 2013.

Newman, P. A. and Nash, E. R.: The unusual Southern Hemisphere stratosphere winter of 2002, Journal of the Atmospheric Sciences, 62, 614–628, 2005.

Palmeiro, F. M., Calvo, N., and Garcia, R. R.: Future changes in the Brewer–Dobson circulation under different greenhouse gas concentrations in WACCM4, Journal of the Atmospheric Sciences, 71, 2962–2975, 2014.

https://doi.org/10.5194/acp-2020-262
Preprint. Discussion started: 16 April 2020

Atmospheric Chemistry and Physics Discussions

Ploeger, F., Abalos, M., Birner, T., Konopka, P., Legras, B., Müller, R., and Riese, M.: Quantifying the effects of mixing and residual circulation on trends of stratospheric mean age of air, Geophysical Research Letters, 42, 2047–2054, 2015.

Ploeger, F., Legras, B., Charlesworth, E., Yan, X., Diallo, M., Konopka, P., Birner, T., Tao, M., Engel, A., and Riese, M.: How robust are stratospheric age of air trends from different reanalyses?, Atmospheric Chemistry and Physics, 2019.

Plumb, R. A.: Stratospheric transport, Journal of the Meteorological Society of Japan. Ser. II, 80, 793–809, 2002.

Polvani, L. M., Abalos, M., Garcia, R., Kinnison, D., and Randel, W. J.: Significant Weakening of Brewer-Dobson Circulation Trends Over the 21st Century as a Consequence of the Montreal Protocol, Geophysical Research Letters, 45, 401–409, 2018.

Prignon, M., Chabrillat, S., Minganti, D., O'Doherty, S., Servais, C., Stiller, G., Toon, G. C., Vollmer, M. K., and Mahieu, E.: Improved FTIR retrieval strategy for HCFC-22 (CHClF2), comparisons with in situ and satellite datasets with the support of models, and determination of its long-term trend above Jungfraujoch, Atmospheric Chemistry and Physics Discussions, 2019.

Randel, W. J. and Newman, P. A.: The stratosphere in the Southern Hemisphere, in: Meteorology of the Southern Hemisphere, pp. 243–282, Springer, 1998.

Randel, W. J., Boville, B. A., Gille, J. C., Bailey, P. L., Massie, S. T., Kumer, J., Mergenthaler, J., and Roche, A.: Simulation of stratospheric N2O in the NCAR CCM2: Comparison with CLAES data and global budget analyses, Journal of the atmospheric sciences, 51, 2834–2845, 1994.

Ray, E. A., Moore, F. L., Rosenlof, K. H., Davis, S. M., Sweeney, C., Tans, P., Wang, T., Elkins, J. W., Bönisch, H., Engel, A., et al.: Improving stratospheric transport trend analysis based on SF6 and CO2 measurements, Journal of Geophysical Research: Atmospheres, 119, 14–110, 2014.

Richter, J. H., Sassi, F., and Garcia, R. R.: Toward a physically based gravity wave source parameterization in a general circulation model, Journal of the Atmospheric Sciences, 67, 136–156, 2010.

Rienecker, M. M., Suarez, M. J., Gelaro, R., Todling, R., Bacmeister, J., Liu, E., Bosilovich, M. G., Schubert, S. D., Takacs, L., Kim, G.-K., et al.: MERRA: NASA Ž019s modern-era retrospective analysis for research and applications, Journal of climate, 24, 3624–3648, 2011.

Scaife, A. and James, I.: Response of the stratosphere to interannual variability of tropospheric planetary waves, Quarterly Journal of the Royal Meteorological Society, 126, 275–297, 2000.

Seinfeld, J. H. and Pandis, S. N.: Atmospheric chemistry and physics: from air pollution to climate change, John Wiley & Sons, 2016.

Seviour, W. J., Butchart, N., and Hardiman, S. C.: The Brewer–Dobson circulation inferred from ERA-Interim, Quarterly Journal of the Royal Meteorological Society, 138, 878–888, 2012.

Shepherd, T. G.: Transport in the middle atmosphere, Journal of the Meteorological Society of Japan. Ser. II, 85, 165–191, 2007.

Solomon, S., Kinnison, D., Bandoro, J., and Garcia, R.: Simulation of polar ozone depletion: An update, Journal of Geophysical Research: Atmospheres, 120, 7958–7974, 2015.

Stiller, G. P., Fierli, F., Ploeger, F., Cagnazzo, C., Funke, B., Haenel, F. J., Reddmann, T., Riese, M., and Clarmann, T. v.: Shift of subtropical transport barriers explains observed hemispheric asymmetry of decadal trends of age of air, Atmospheric Chemistry and Physics, 17, 11 177–11 192, 2017.

Strahan, S., Oman, L., Douglass, A., and Coy, L.: Modulation of Antarctic vortex composition by the quasi-biennial oscillation, Geophysical Research Letters, 42, 4216–4223, 2015.

Strahan, S. E., Douglass, A., Stolarski, R., Akiyoshi, H., Bekki, S., Braesicke, P., Butchart, N., Chipperfield, M., Cugnet, D., Dhomse, S., et al.: Using transport diagnostics to understand chemistry climate model ozone simulations, Journal of Geophysical Research: Atmospheres, 116, 2011.

https://doi.org/10.5194/acp-2020-262
Preprint. Discussion started: 16 April 2020

Atmospheric Chemistry and Physics Discussions

Tweedy, O., Waugh, D., Stolarski, R., Oman, L. D., Randel, W., and Abalos, M.: Hemispheric differences in the annual cycle of tropical lower stratosphere transport and tracers, Journal of Geophysical Research: Atmospheres, 122, 7183–7199, 2017.

Waugh, D. W. and Randel, W. J.: Climatology of Arctic and Antarctic polar vortices using elliptical diagnostics, Journal of the Atmospheric Sciences, 56, 1594–1613, 1999.

Yamazaki, Y., Matthias, V., Miyoshi, Y., Stolle, C., Siddiqui, T., Kervalishvili, G., Laštovička, J., Kozubek, M., Ward, W., Themens, D. R., et al.: September 2019 Antarctic sudden stratospheric warming: quasi-6-day wave burst and ionospheric effects, Geophysical Research Letters, 2019.